Natriuretic Peptide Signaling Acts Throughout Life to Maintain Spinal Straightness in Zebrafish

by

Hannah Markovic

A dissertation accepted and approved in partial fulfillment of the

requirements for the degree of

Doctor of Philosophy

in Biology

Dissertation Committee:

Karen Guillemin, Chair

Kryn Stankunas, Advisor

John Postlethwait, Core Member

Kenneth Prehoda, Institutional Representative

University of Oregon

Spring 2026

© 2026 Hannah Markovic

DISSERTATION ABSTRACT

Hannah Markovic

Doctor of Philosophy in Biology

Title: Natriuretic Peptide Signaling Acts Throughout Life to Maintain Spinal Straightness in Zebrafish

To improve detection methods and treatments for spinal curves, it is necessary to understand how the spine develops and maintains its shape. Here, we use zebrafish to investigate how natriuretic peptide signaling maintains a straight spine.

C-type Natriuretic Peptide (CNP) is a small peptide known to regulate bone growth. Mutations in humans which increase CNP signaling result in tall stature and spinal curves, whereas decreased CNP signaling causes dwarfism. Work in mice identified that CNP may regulate chondrocyte differentiation, but how CNP signaling maintains spinal straightness is not understood.

We generated zebrafish mutants for *nppc* (encoding CNP) and two natriuretic peptide receptors, *npr1b* and *npr3*. We found that adult *npr1b*$^{-/-}$ and *npr3*$^{-/-}$ fish had spinal curves. We performed microCT scanning and identified changes in vertebral shape in these mutants. We used calcein staining to investigate vertebral development and found that *npr1b*$^{-/-}$ mutants had delayed vertebral calcification at 7 - 15 days post fertilization (dpf) but developed spinal curves during juvenile growth phases (15 dpf - 3 months old). In contrast, *npr3*$^{-/-}$ fish developed caudal spine curves at early stages, but vertebral fusions occurred during juvenile growth. We found that cerebrospinal fluid-contacting neurons (CSF-cNs), which are essential for developing and maintaining a straight spine, co-expressed *nppc*, *npr1b*, and *npr3*. We identified no changes in notochord segmentation or cell number in *npr1b* or *npr3* mutants, but found decreased collagen

II around the notochord sheath in *npr1b*$^{-/-}$ larvae. This suggests that natriuretic peptide signaling promotes collagen expression. Finally, we observed accelerated rates of aging-related kyphosis in *nppc*$^{-/-}$ and *npr1b*$^{-/-}$ fish. We conclude that natriuretic peptide signaling has multiple roles throughout life in developing and maintaining a straight spine.

I additionally assessed whether CNP is involved in caudal fin regeneration. I identified expression of CNP and its receptors in caudal fin tissues. *Npr1b* mutants regenerated shorter caudal fins. Additionally, I observed that some *npr1b*$^{-/-}$*;npr3*$^{-/-}$ double mutants had extremely short fins, suggesting that these receptors may work together to promote fin growth.

This dissertation includes unpublished co-authored material.

ACKNOWLEDGMENTS

First, I want to thank my advisor, Kryn Stankunas, who was extremely understanding of my health conditions. He helped me seek accommodations and funding, plan experiments, and coordinate with other lab members so that I was able to finish this PhD in spite of disabilities.

I also want to thank Scott Stewart for his mentorship and support.

I want to acknowledge Astra Henner for her contributions to numerous experiments over the past few years. I would not have been able to complete this dissertation without her help easing back into lab work after my medical leave.

I want to thank Beth Bearce for collaborating with me on this project. Her expertise in microCT imaging was a great help, and those experiments are essential to my dissertation and manuscript in preparation. This work would not have the impact it does without her contributions.

Finally, I want to thank all the Stankunas lab members over the years for their support and companionship.

DEDICATION

This dissertation is dedicated to my family.

TABLE OF CONTENTS

Chapter Page

I. INTRODUCTION 11

Co-Author Contributions 11

Background 12

Bridge 14

II. NATRIURETIC PEPTIDE SIGNALING AND THE ZEBRAFISH SPINE 15

Introduction 15

Materials & Methods 19

Results 27

Loss of natriuretic peptide receptors in zebrafish leads to spinal curves 27

Loss of both *npr1b* and *npr3* compounds spinal phenotypes 31

Vertebral changes in *npr1b* and *npr3* mutants begin during larval development 32

Nppc, *npr1b*, and *npr3* are expressed in the spinal cord and notochord during vertebral development 34

Natriuretic peptide signaling promotes expression of bone components 36

CNP signaling is essential for maintaining spinal straightness during aging 38

Discussion 40

Bridge 43

III. NATRIURETIC PEPTIDE SIGNALING IN FIN REGENERATION 44

Introduction 44

Materials & Methods 47

Chapter Page

Results 49

CNP and its receptors are expressed in regenerating caudal fins 49

Fish lacking *npr1b* regenerate slightly shorter caudal fins 51

Discussion 53

Bridge 56

IV. CONCLUDING SUMMARY 57

Summary 57

Unanswered Questions 59

Concluding Thoughts 61

REFERENCES CITED 62

LIST OF FIGURES

Figure Page

1. Loss of *npr1b* or *npr3* causes spinal curves in adult zebrafish 28
2. Craniofacial structures develop normally in *npr1b* and *npr3* mutants 30
3. Combined loss of *npr1b* and *npr3* in females causes dwarfism 31
4. *Npr1b* and *npr3* are essential for proper vertebral development 33
5. Natriuretic peptide pathway components are expressed within the spinal cord and notochord..... 35
6. Natriuretic peptide receptors control expression of bone components rather than notochord segmentation 37
7. *Nppc* and *npr1b* prevent aging-related kyphosis 38
8. CNP and its receptors are expressed in the developing and regenerating caudal fin..... 49
9. *Npr1b* mutants regenerate slightly shorter fins 52

LIST OF TABLES

Table Page

1. Guide RNA Sequences 19

2. Injection Mixes 20

3. PCR Primer Sequences 23

CHAPTER I. INTRODUCTION

Co-Author Contributions

Chapter II comprises work from my manuscript in preparation, which will be preprinted and submitted for publication this summer. The manuscript authors are myself, Elizabeth A. Bearce, Scott Stewart, Daniel T. Grimes, and Kryn Stankunas.

Chapter III comprises solely my own work.

Background

Zebrafish, like most fish, are remarkably adept at regenerating their organs. The Stankunas lab uses the zebrafish fin as a model for bone regeneration. Accordingly, we initially became interested in natriuretic peptide signaling in the context of fin bone regeneration. We noted that increases in C-type Natriuretic Peptide (CNP) signaling in humans causes tall stature, while decreased CNP signaling results in dwarfism, suggesting a role in regulating bone size (Bartels et al., 2004; Boudin et al., 2019; Hachiya et al., 2007; Hannema et al., 2013; Khan et al., 2012; Lauffer et al., 2022; Miura et al., 2012; Miura et al., 2014; Moffatt et al., 2025; Olney et al., 2005; Vasquez et al., 2013). We wondered whether CNP also controls bone scaling in the zebrafish fin. I used our single-cell RNA sequencing dataset (Lewis et al., 2023) to determine that the genes *nppc* (encoding CNP), *npr1b* (encoding natriuretic peptide receptor 1b (Npr1b)), and *npr3* (encoding Npr3) are expressed in regenerating fin mesenchyme.

We successfully generated zebrafish mutants for each of these genes. Surprisingly, fins developed normally. We performed fin regeneration experiments in each mutant line, but only *npr1b*$^{-/-}$ fish had a significant regenerative phenotype (see chapter III). Compared to other mutants we work with, *npr1b* only had a small effect on regenerated length, implying that its role in fin regeneration is relatively unimportant. We decided that it was not worthwhile to continue investigating fin regeneration in these mutant lines. However, the two natriuretic peptide receptor mutants had spinal curves – and zebrafish are excellent models for the study of scoliosis. *Npr1b*$^{-/-}$ and *npr3*$^{-/-}$ zebrafish are also excellent disease models because increased CNP signaling, including through loss of NPR-C (zebrafish Npr3), is associated with spinal curves in human patients (Bocciardi et al., 2007; Hannema et al., 2013; Miura et al., 2012; Miura et al., 2014; Moffatt et al., 2025). Therefore, rather than abandoning this project, I pivoted to investigating

spinal curves in these mutants. I had the luxury of collaborating with the Grimes lab next door, who are experts in the study of spinal straightness and CSF-contacting neurons. Although this project progressed in an unexpected direction, I was nevertheless able to apply my microscopy and developmental biology skills and generate a satisfactory body of work. I examined the role of natriuretic peptide signaling in bone growth and maintenance across life stages and even began to probe at the mechanisms behind its action. This project not only establishes zebrafish as a model of CNP-related spinal curves, but also opens the doors to studying numerous questions about spinal development and maintenance, including how neurons may transduce information about spinal straightness into signals to correct spinal curves.

Bridge

In the next chapter, I will discuss the role of natriuretic peptide signaling in vertebral development and maintenance of a straight spine, which was the bulk of my PhD work. As this chapter comprises work from my manuscript in preparation, it is introduced from the perspective of spinal development. I will discuss my findings on the role of CNP in fin regeneration in chapter III.

CHAPTER II. NATRIURETIC PEPTIDE SIGNALING AND THE ZEBRAFISH SPINE

This chapter contains material from my manuscript in preparation. The manuscript authors, in order, are myself, Elizabeth A. Bearce, Scott Stewart, Daniel T. Grimes, and Kryn Stankunas. EAB performed micro-Computed Tomography scanning and analyses. SS designed and synthesized guide RNAs for the mutant alleles generated here. All authors contributed to experiment design and to manuscript editing. I wrote the manuscript and performed all other experiments and data analyses.

Introduction

A straight spine is established early in vertebrate development and is maintained while the animal grows and progresses through adulthood. Errors in the development and maintenance of symmetric and distinct vertebrae, or in their alignment, can result in spinal curves. Spinal curves can be a congenital defect but may also arise during adolescence or aging. C-type Natriuretic peptide signaling regulates bone growth and is genetically linked to human spine curvature abnormalities. However, the mechanistic roles of natriuretic peptides in vertebral development and spine straightening are unresolved. We leveraged the zebrafish model to explore when and how natriuretic peptide signaling influences vertebral development and thereby contributes to the establishment and maintenance of a straight spine.

Natriuretic peptides are best known for their roles in cardiovascular development, natriuresis, and blood pressure regulation. A-type, B-type, and C-type natriuretic peptides (ANP, BNP, and CNP, respectively) share similar structures and signal through natriuretic peptide receptors, which have species-dependent affinities (Suga et al., 1992). Binding to natriuretic

peptide receptors NPR-A or NPR-B activates guanylyl cyclase domains, producing cyclic GMP. The third receptor, NPR-C, lacks a guanylyl cyclase domain and is thought to limit pathway activity through receptor-mediated endocytosis (Cohen et al., 1996), although NPR-C can also inhibit adenylyl cyclase activity via G_i signaling (Anand-Srivastava et al., 1990; Anand-Srivastava *et* al., 1996; Pagano & Anand-Srivastava, 2001).

While ANP and BNP largely fulfill the cardiovascular roles of natriuretic peptide signaling, CNP signaling is linked to long bone growth, stature, and scoliosis. In humans, loss-of-function mutations in NPR-B cause short stature and disproportionate dwarfism (Bartels et al., 2004; Hachiya et al., 2007; Khan et al., 2012; Olney et al, 2005; Vasquez et al., 2013). In contrast, activating mutations in NPR-B result in tall stature as well as scoliosis or kyphosis (Hannema et al., 2013; Miura et al., 2012; Miura et al., 2014). Similarly, loss-of-function of the clearance receptor NPR-C causes tall stature and long digits (Boudin et al., 2018; Lauffer et al., 2022;) and is associated with scoliosis (Moffatt et al., 2025). Increased CNP expression due to a chromosome translocation also causes bone overgrowth and scoliosis (Bocciardi et al., 2007). Overall, increases in CNP signaling cause tall stature and spinal curves in humans, whereas decreased CNP signaling results in short stature.

Mouse models largely phenocopy human conditions and indicate that CNP signaling regulates chondrocyte differentiation. *Nppc*$^{-/-}$ and *Npr2*$^{-/-}$ mice have reduced body length with decreased hypertrophic and proliferative chondrocytes in tibia growth plates (Chusho et al., 2001; Sogawa et al., 2007; Tamura et al., 2004; Tsuji & Kuneida, 2005). In contrast, *Npr3*$^{-/-}$ mice have long bodies, enlarged vertebrae, and kyphosis, accompanied by expansion of hypertrophic chondrocytes in limb and vertebral growth plates (Dauphinee et al., 2013; Esapa et al., 2016; Jaubert et al., 1999; Matsukawa et al., 1999). Overexpression of BNP or CNP similarly leads to

elongated limbs and kyphosis (Bocciardi et al., 2007; Suda et al., 1998). However, how CNP signaling influences vertebral development, spinal alignment, or their maintenance over time remains unresolved.

Across vertebrates, spinal straightness depends on initial axial patterning and later stages of vertebral growth and maturation. Maintaining straight alignment of vertebral segments involves coordinated vertebral expansion, matrix deposition, mineralization, and restraint of aberrant growth that otherwise can lead to fusions or curvature. In teleosts, vertebral centra form through mineralization of the notochord sheath followed by growth of surrounding skeletal tissues (Wopat et al., 2018). Cerebrospinal fluid-contacting neurons (CSF-cNs) that line the central canal of the spinal cord contribute to spine straightness by detecting spinal curvature with their primary cilia and respond, in part, by releasing urotensin-related peptides which may signal to axial muscles (Bearce et al., 2022; Lu et al., 2020; Sternberg et al., 2018; Zhang et al., 2018). Natriuretic peptide pathway components *nppc* and *npr3* are also expressed in CSF-cNs in zebrafish (Prendergast et al., 2023), raising the possibility that natriuretic peptide signaling may be another mechanism by which CSF-cNs act to maintain and establish a straight spine.

We took advantage of the optical and genetic tractability of zebrafish to examine the roles of natriuretic peptide signaling in vertebral development and spinal straightness across life stages. We established mutant alleles for *nppc, npr1b,* and *npr3*. Loss of *npr1b* or *npr3* led to spinal curvature in adult zebrafish. We found vertebral calcification delays in *npr1b*$^{-/-}$ larvae, with spinal curves arising during later juvenile growth and in the absence of overt vertebral malformations. In contrast, *npr3*$^{-/-}$ larvae developed a characteristic caudal spine kink during vertebral calcification, with vertebral fusions and corresponding mid-spine curves emerging during juvenile growth. Normal notochord sheath segmentation but altered collagen II protein

levels suggest that natriuretic signaling influences vertebral matrix production or mineralization dynamics rather than cell differentiation or patterning. A new *nppc:nls-Eos* knock-in reporter line confirmed *nppc* expression in spinal neurons and vertebral arches during larval stages. Finally, accelerated aging-related kyphosis in *nppc* and *npr1b* mutants indicates that natriuretic peptide signaling also acts to maintain spinal straightness later in life. Our findings link natriuretic peptide signaling to vertebral maturation and to maintenance of spinal morphology throughout life.

Materials & Methods

Zebrafish husbandry

Zebrafish were housed under standard conditions by the University of Oregon Aquatic Animal Care Services (Lawrence and Mason, 2012). Embryos and larvae were housed in petri dishes, with feeding of larvae beginning at 5 days post fertilization (dpf). At 11 dpf, larvae were moved to nursery tanks, unless being held in beakers for an experiment. Juvenile fish were moved to standard housing tanks at 3-4 weeks post fertilization.

Generation of mutant alleles

CRISPR-Cas9 mutagenesis was used to generate zebrafish mutant alleles for *nppc*, *npr1b*, and *npr3*. Guide RNAs (Table 1) were designed using CHOPCHOP v3 (Labun et al., 2019) to be approximately 100 base pairs apart and flanking the start codon. Guide RNA pairs, along with Cas9 protein and Phenol Red for visualization, were injected into AB line wild type zebrafish embryos. Approximately 2 nL of injection mix (Table 2) was injected at the one-cell stage using a pulled capillary tube needle and microinjector rig. Injected embryos were grown to

Table 1. Guide RNA Sequences

Guide RNA	Nucleotide Sequence
nppc (1)	CCATCACCATGATCATCTCGCAT
nppc (2)	CCTCTGACACAGGCTGAACAGAG
npr1b (1)	CCTGGACCAAGATCAGCAAACAC
npr1b (2)	CCCCAATCTGCTGCCCCGGCACC
npr3 (1)	CCACTCTGTCTGTCCATTTGGGC
npr3 (2)	CCTCGCAACAACACATACCTGTT
mBait	CCACCTCTGGAACCGCAGCAGCC

Table 2. Injection Mixes

Components	Final concentration (for mutant lines)	Final concentration (for *nppc:nls-Eos* knockin)
Cas9 protein	500 ng/μL	500 ng/μL
gRNA 1	100 ng/μL	100 ng/μL
gRNA 2	100 ng/μL	100 ng/μL
mBait gRNA	/	200 ng/μL
Eos plasmid	/	16.7 ng/μL
Phenol red if desired for visualization		
RNAse-free water		

adulthood, after which they were crossed to wild type fish. F_1 progeny were genotyped to screen for germline-transmitted mutations.

Adult and aged fish photography

Fish were anesthetized in 0.17 g/L tricaine solution and placed on a sheet of white plastic in a Styrofoam light box. A light source was positioned through a hole in the right side of the light box. Fish were positioned on the plastic surface using a paintbrush. A ruler was placed adjacent to them, and they were photographed using a Fujifilm X-A1 digital camera. To photograph body curves from the dorsal view, fish were gently pushed upright with the paintbrush so that they balanced on their stomachs. The imaging was completed within a few minutes, and fish were quickly placed in a recovery tank and monitored while breathing restarted.

Standard length was measured using FIJI (ImageJ) software. The ruler in the photograph was used to set the scale of pixels to cm. Then, the straight line tool was used to measure standard length, from the tip of the jaw to the caudal peduncle.

Aged zebrafish were photographed using the same method as adult mutant photography above. *Nppc* homozygous mutant and heterozygous zebrafish were imaged at 13, 15, 16, and 18 months post-fertilization. Individual fish were tracked between time points by gender and pigmentation pattern. *Npr1b* and *npr3* homozygous mutants and heterozygous controls were imaged at 18 months of age.

MicroCT imaging

Micro-Computed Tomography (microCT) scanning was performed on 4 to 5 month old adult mutant zebrafish. Representative adult fish were selected and separated by genotype and sex. They were euthanized by overdose in tricaine solution and fixed in 4% paraformaldehyde at 4°C. For imaging, fish were suspended in agarose within conical centrifuge tubes. Scans were thresholded and 3D models generated for viewing and further analysis. The same process was repeated for aged *nppc* mutants and heterozygous siblings.

Alcian blue/alizarin red staining

Alcian blue and alizarin red combined staining was performed following a standard protocol ("Kimmel lab no acid bone & cartilage stain for larval fish," modified from Walker & Kimmel, 2007). 9 or 10 dpf AB line wild type and homozygous mutant larvae were anesthetized in tricaine solution and sorted by standard length. Larvae were then euthanized by tricaine overdose, fixed in 4% PFA, and stained with alcian blue and alizarin red. Larvae were imaged within 5 hours post-staining with a Leica dissecting microscope. Stained larvae were mounted in low-melt agarose in the sagittal view and a transparent ruler placed under the sample dish.

Samples were imaged with brightfield illumination. Larvae were removed from agarose and re-mounted in the coronal view for additional imaging. Wild type controls and mutant samples were alternated to account for quick fading of alizarin red. ImageJ software was used to set image scales based on the ruler and to measure standard length using the straight line segment tool.

Calcein staining

Calcein fluorescent dye, which binds to Ca^{2+} ions, was used to assess vertebral development in *nppc*, *npr1b*, and *npr3* mutants (as in Xi et al., 2013). Homozygous and heterozygous mutant fish were crossed to generate heterozygous and homozygous mutant siblings. Larvae to be stained at 7, 9, or 11 dpf were fasted for two days prior to imaging to minimize autofluorescence of gut contents. As feeding begins at 4-5 dpf, larvae for 7 dpf staining were never fed. Fasting was also not performed for larvae stained at 13 or 15 dpf due to lethality. Larvae were collected at 7, 9, 11, 13, and 15 dpf time points and stained in 0.2% Calcein green in Embryo Media (EM) for 10 minutes (Grimes Lab, n.d.). Three washes in EM were performed. Larvae were then anesthetized in tricaine solution, mounted in 1% low melting point agarose (16520-100, Invitrogen) in a FluoroDish™ (FD35-100, World Precision Instruments), and imaged using a Nikon spinning disk microscope. Following imaging, larvae were euthanized in excess tricaine and genotyped using PCR (Table 3).

ImageJ software was used to modify brightness and contrast, generate z projections, and to count calcein-stained vertebral centra. The calcein stain was inherently variable in intensity and therefore representative images in Figure 3 were *not* adjusted to the same brightness to aid in viewing. The multipoint tool was used to count mineralizing centra, visible as rectangular (cylindrical in 3D space) fluorescent domains within the notochord. Smaller puncta, representing the beginning stages of centra mineralization, were also included in the count if they were

positioned within the notochord and at the correct spacing from other centra. A single z slice, where the posterior notochord was in focus, was isolated and used to measure standard length in each fish. The straight line tool was positioned with the ends at the tip of the upper jaw and at the posterior end of the notochord, and the length recorded.

Table 3. PCR Primer Sequences

PCR target	Primers	Annealing Temperature (°C)
*nppc**	CTGGTGTGACGTCACAGGAGTG	60
	CTCATTCACACTTTTATCGAACGTCAATAAAGCC	
npr1b	TCAGTTGGAAGTGTGAGCTGCA	61
	AGCTGTGATCATGGGGAGGCCC	
npr3	GGGCTCTGGACACACTTGCAGG	69
	GTCTTTCTGCCGGTCCACGAGC	
npr3 (for $npr3^{b-}$ allele)†	AGGCAAGAGAGAGAGAGGGAGA	67
	CAGTGCACTTGTCCTGCCAGGC	
nppc:nls-Eos insertion	AGCCGATGCGGGAAGAGGTGTA	60
	CTCATTCACACTTTTATCGAACGTCAATAAAGCC	

*Both alleles disrupt a cut site for enzyme Hpy188I. PCR was digested overnight at 37°C. Wild type band sizes are 217, 124, and 39 bp. Mutant band sizes are 217 and 163 bp.

†This allele was genotyped using a re-annealing method for small deletions (Bhattacharya & Van Meir, 2019).

Nppc:nls-Eos line generation

A nuclear-localized Eos fluorescent protein reporter under control of endogenous *nppc* promoter was generated, referred to as *nppc:nls-Eos*. An injection mix consisting of the two guide RNAs (gRNA) targeting *nppc*, mBait gRNA, Eos plasmid containing mBait sequence, Cas9 protein, and Phenol Red was injected into 1-cell stage, AB line wild type embryos at approximately 2 nL per embryo (Tables 1, 2). Injected embryos were grown to adulthood and crossed to wild type fish, with progeny screened for Eos fluorescence between 1-5 dpf. An F_0 founder was identified, its progeny grown to adulthood, and a single F_1 founder with fluorescent progeny selected to establish the line. Insertion in the *nppc* locus was verified by PCR across the insertion site and PCR product sequencing (not shown; primers in Table 3).

Nppc:nls-Eos in vivo fluorescent imaging

8, 12, and 15 dpf *nppc:nls-Eos/+; Tg[entpd5a:pkRed]*^{hu7478} /+ (Wopat *et al.*, 2018) larvae were imaged to assess *nppc* expression. Larvae were raised as normal in our fish facility nursery until they reached the desired age. Larvae were then transferred into a petri dish, anesthetized in tricaine solution, and mounted in a FluoroDish^{TM} (FD35-100, World Precision Instruments) using 1% low melting point agarose (16520-100, Invitrogen) containing 1 drop of 4.0 g/L tricaine per 1 mL of agarose. Larvae were imaged using a Nikon spinning disk microscope. Due to optical working distance limitations, only the closer half of vertebrae was imaged at higher magnifications. ImageJ software was used to measure standard length using the straight line tool, adjust brightness and contrast levels, and to generate maximum intensity projections.

Nppc:nls-Eos larval section immunofluorescence

Paraffin blocks were generated and sections immunostained as previously described, using 10 dpf *nppc:nls-Eos/+* larval zebrafish rather than caudal fin tissue (Stewart & Stankunas,

2024). Sagittal and transverse sections passing through the spinal canal were chosen for staining. Sections were incubated in 1:5000 Eos antibody (RPCA-EosFP; EnCor Biotechnology Inc.), 1:100 pan-cadherin antibody (NBP1-22631; Novus), 1:250 acetylated tubulin antibody (GTX11323; Genetex), and finally stained with 3.3 mg/L Hoechst 33342 to visualize nuclei. Imaging was performed using a Nikon spinning disk microscope. ImageJ software was used to modify brightness and contrast, and to generate composite fluorescent images.

RNAScope

The RNAScope Multiplex Fluorescent kit (ACD Bio) was used to assess *nppc, npr1b,* and *npr3* expression in larval tissue sections. 10 dpf wild type or *nppc:nls-Eos/+* larvae were processed, embedded in parrafin blocks, and sectioned. Probes were designed for *nppc, npr1b,* and *npr3* mRNA by ACD Bio. Slides were processed according to kit recommendations. Hoechst stain was used to visualize nuclei. Samples were imaged on a Nikon spinning disk microscope and images processed using ImageJ software.

***Entpd5a:pkRed* imaging**

The *Tg[entpd5a:pkRed]*^{hu7478} mineralizing cell reporter line (Wopat et al., 2018) was used to assess potential changes in notochord or osteoblast cell number in *npr1b* and *npr3* larval homozygous mutants and heterozygous controls. Homozygous and heterozygous mutant adult zebrafish were crossed to generate a mix of homozygous and heterozygous siblings. Larvae were raised as normal in our fish facility nursery until they reached 10 dpf. Larvae were then moved into a petri dish, anesthetized in tricaine solution, and mounted in a small FluoroDish^{TM} using 1% low melting point agarose. Brightfield stitched images were taken to later measure standard length of each larva. A Nikon spinning disk microscope was used to take z-stack images of pkRed fluorescence of the entire larva, and of select vertebrae at higher resolution (vertebrae 1-7

and 15-19). After imaging, larvae were removed from agarose, placed in PCR wells, and euthanized by tricaine overdose. Larval tissue was lysed and used to genotype each imaged larva by PCR. ImageJ software was used to measure standard length using the straight line tool, adjust brightness and contrast levels, and to generate maximum intensity projections.

Whole-mount immunofluorescence on 8-10 dpf zebrafish larvae

In brief, larval zebrafish were collected at 8-10 dpf, fixed in paraformaldehyde, and transferred to methanol for storage at -20°C. Proteinase K digestion (50 µg/mL for 1 hour) was used to improve antibody penetration into the tissue (modified from Thisse & Thisse, n.d.). Larvae were fixed in paraformaldehyde to halt digestion and blocked in Bovine Serum Albumin (CAS 9048-46-8, Fisher Scientific). Larvae were then incubated in 1:100 Col2a1 antibody (II-II6B3, DSHB), washed, and incubated in secondary antibody. Finally, larvae were stained with 3.3 mg/L Hoechst 33342 and stored in 50% glycerol/1x PBS at 4°C. Larvae were mounted in low-melt agarose in a small FluoroDish^{TM} and imaged using a Nikon spinning disk microscope. Vertebrae 5 and 18 were imaged from the lateral edge to the center of the notochord (passing through half of the spinal canal and notochord volume) using the central canal and surrounding cells as guides. ImageJ software was used to adjust brightness and contrast, and to generate maximum intensity z projections.

Results

Loss of natriuretic peptide receptors in zebrafish leads to spinal curves

We began by establishing mutant lines to test whether CNP signaling controls vertebral bone development in zebrafish, as it does in mammals. We generated putative loss-of-function alleles for *nppc* (encoding CNP), *npr1b* (encoding Npr1b, homologous to NPR-A) and *npr3* (encoding Npr3, homologous to NPR-C) using CRIPSR-Cas9 mutagenesis. Adult *nppc*$^{-/-}$ fish appeared overtly normal, but *npr1b*$^{-/-}$ and *npr3*$^{-/-}$ fish developed spinal curves (Figure 1A). *Npr1b* mutants occasionally developed a permanent head tilt and/or mild curves in other spinal regions (Figure 1A, arrowheads). All *npr3* mutants developed a severe curve in the posterior-most spine, likely within caudal fin vertebrae, and occasionally developed kinks in the mid-spine (Figure 1C, C'). As human mutations in this pathway may lead to either dwarfism or increased stature (Bartels *et al.*, 2004; Bocciardi *et al.*, 2007; Boudin *et al.*, 2018; Hachiya *et al.*, 2007; Hannema *et al.*, 2013; Khan *et al.*, 2012; Lauffer *et al.*, 2022; Miura *et al.*, 2012; Miura *et al.*, 2014; Olney *et al.*, 2005; Vasques *et al*., 2013), we also assessed standard length, a measure of body size in fish. We found that *nppc*$^{-/-}$, *npr1b*$^{-/-}$, and *npr3*$^{-/-}$ fish were all significantly shorter than wild type clutchmates, although the magnitude of effect is greatest in *npr1b* mutants (Figure 1B). These results suggest that natriuretic peptide signaling is essential for spinal straightness in zebrafish and support further use of this model to study the role of CNP signaling in vertebral development and in maintaining a straight spine.

We also noted mutant phenotypes in other bony tissues. The heads of *npr1b*$^{-/-}$ and *npr3*$^{-/-}$ fish appeared to be slightly smaller than controls (Figure 1A). The lower jaw of *npr3*$^{-/-}$ fish also appeared to be larger or extended compared to controls (Figure 1A, arrows). In *npr3* mutants, the number of rays and caudal fin morphology appeared normal, but the dorsal lobe of the caudal fin

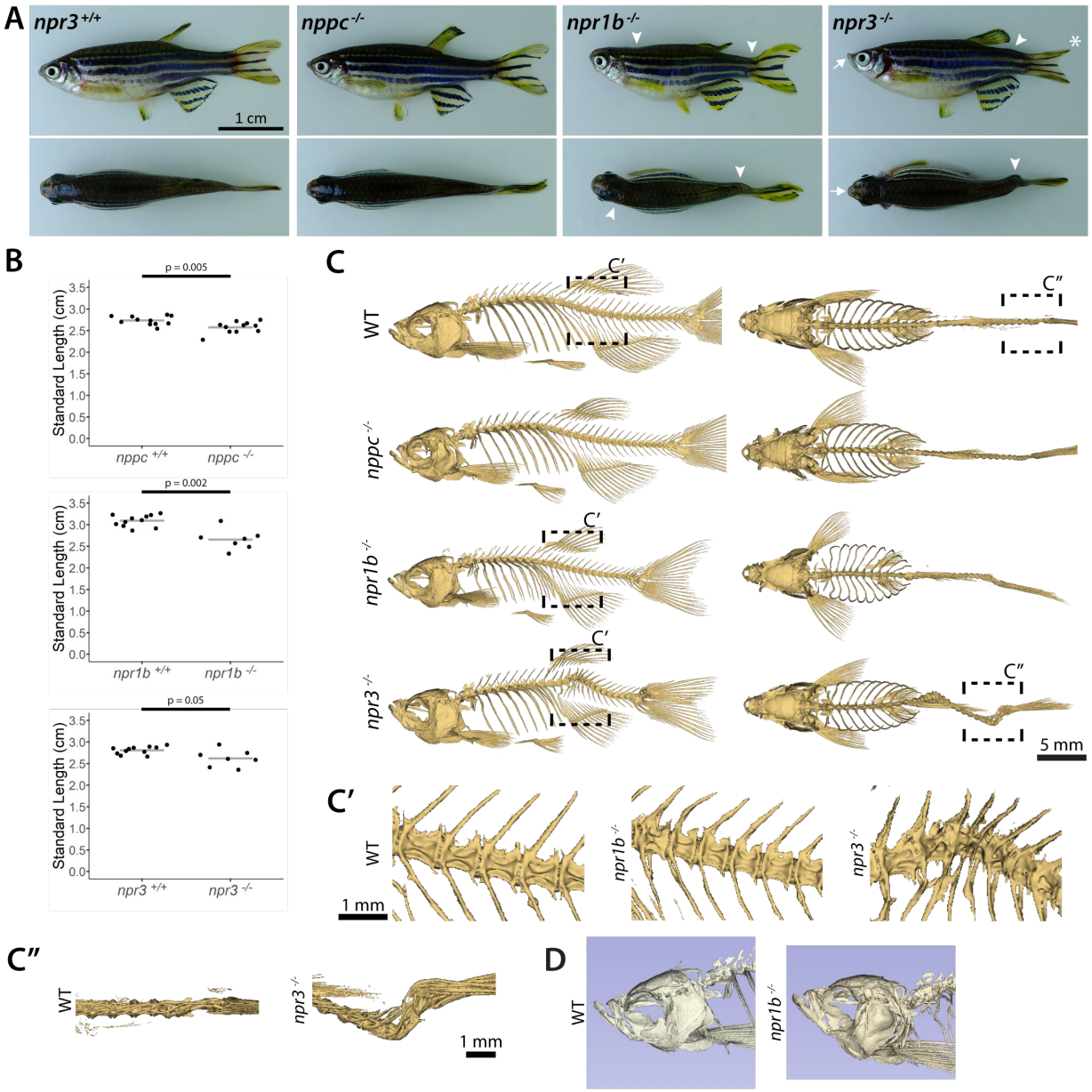


Figure 1. Loss of *npr1b* or *npr3* causes spinal curves in adult zebrafish. At approximately 6 months of age, *npr1b* and *npr3* homozygous mutants have spinal curves (**A**, arrowheads). *Npr3* mutant fish appear to have longer jaws (**A**, arrow) and often have caudal fins with the dorsal lobe folded over itself (**A**, asterisk). *Nppc*$^{-/-}$, *npr1b*$^{-/-}$, and *npr3*$^{-/-}$ fish are significantly shorter than control siblings (**B**). MicroCT scans confirm spinal curves in *npr1b*$^{-/-}$ and *npr3*$^{-/-}$ fish (**C**). Vertebrae in *npr1b*$^{-/-}$ fish appear to be shorter than controls. *Npr3*$^{-/-}$ fish have similarly sized vertebrae as controls, but suffer from stochastic vertebral fusions (**C'**). *Npr3*$^{-/-}$ fish have a consistent, severe kink phenotype in their caudal vertebrae (**B''**). *Npr1b*$^{-/-}$ fish often have skulls fixed at an improper angle to the spine (**D**) N=5 fish were scanned per genotype (WT, *nppc*$^{-/-}$, *npr1b*$^{-/-}$, *npr3*$^{-/-}$), with approximately equal numbers of male and female fish. WT, wild type.

was often folded over itself (Figure 1A, asterisk). Thus, CNP signaling may control development of multiple bone types in zebrafish, in contrast to mammals, where phenotypes are largely confined to the spine.

We performed micro-Computed Tomography (microCT) scanning on *nppc*, *npr1b*, and *npr3* mutants and wild type controls to determine whether body curvatures are due to vertebral changes (Figure 1C - D). We generated spinal traces to compare curve locations across all samples, and assessed spinal cord length. We identified no phenotypes in *nppc* mutants. In *npr1b* mutants, we found mild spinal curves, tilted skulls, and a decreased spinal cord length in comparison to controls (Figure 1C, D). We assessed vertebral shape in *npr1b* mutants and found that *npr1b*$^{-/-}$ fish have vertebrae that are shorter in the anterior-posterior axis (Figure 1C'). *Npr3* mutants also display changes in vertebrae shape. Caudal fin centra were misshapen and fused, resulting in severe caudal spine kinks (Figure 1C''). In addition, we identified vertebral fusions in *npr3* mutants associated with stochastic mid-spine curves (Figure 1C'). We conclude that spinal curves in *npr1b* and *npr3* mutants are due to vertebral shape changes.

We also used the microCT data to investigate potential craniofacial changes in *npr3* mutants. Skulls were isolated from the microCT scans for further analysis. We quantified skull bone volume, density, jaw length, and Meckel's angles (Figure 2A). *Npr1b*$^{-/-}$ skull bone volume was significantly smaller than controls. Surprisingly, we found no changes in jaw length or Meckel's angles even though *npr3*$^{-/-}$ jaws superficially appear longer. In addition, we performed Alcian blue/Alizarin red combined staining on 9-10 dpf *npr1b*$^{-/-}$ and *npr3*$^{-/-}$ larvae to assess craniofacial development and observed no apparent differences (Figure 2B-C). Therefore, *npr3* jaw phenotypes may instead be caused by changes in jaw bone attachment. Overall, our results

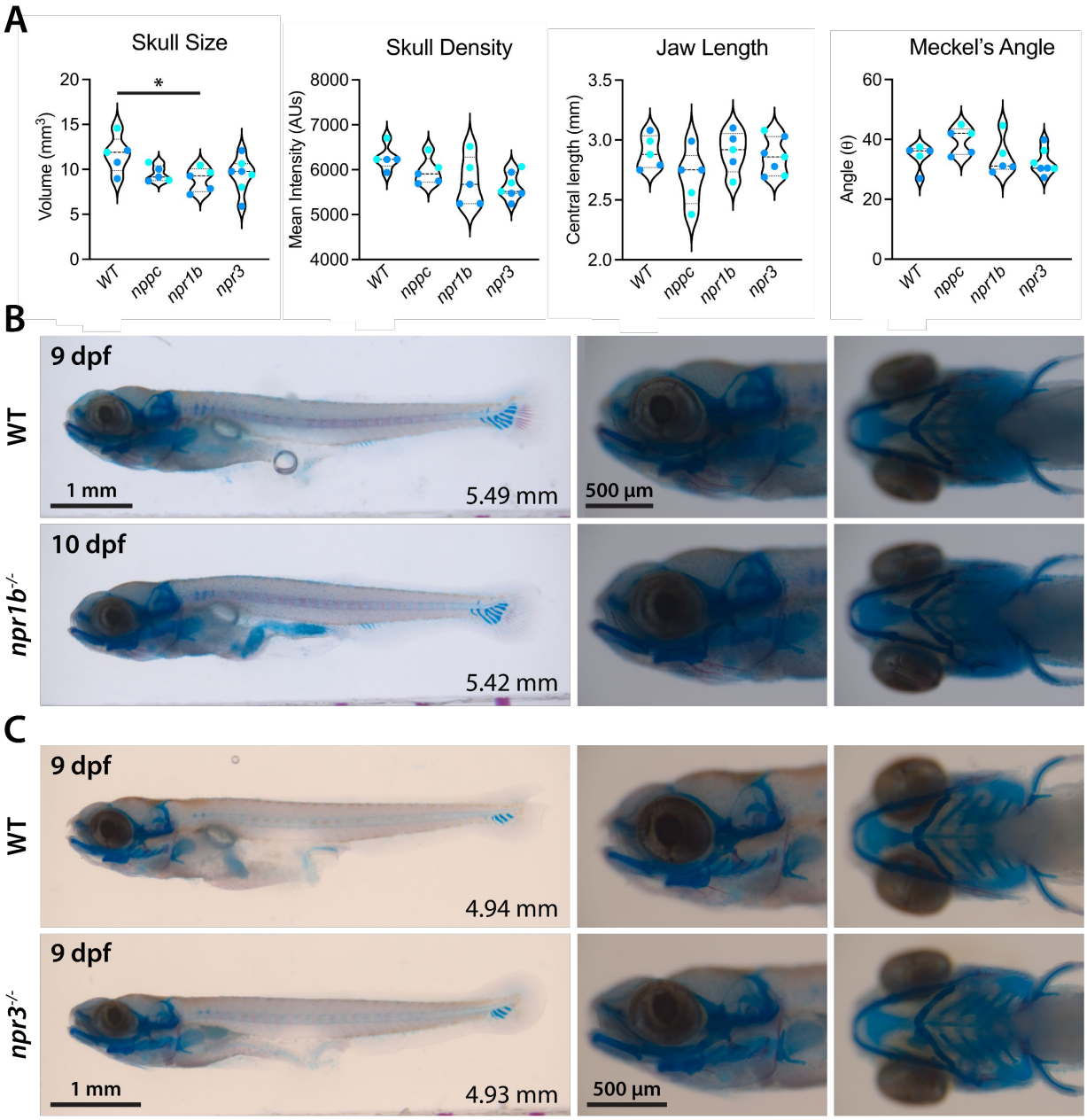


Figure 2. Craniofacial structures develop normally in *npr1b* and *npr3* mutants. Adult microCT skull measurements (**A**). Alcian blue and alizarin red staining for *npr1b* (**B**) and *npr3* (**C**) mutant larvae. As *npr1b* mutants tend to grow more slowly, 10 dpf mutants and 9 dpf WT controls were used to compare fish closer in standard length. *, $p < 0.05$.

mirror mammalian work, where skeletal changes are confined to spinal bones and do not affect craniofacial bone development.

Loss of both *npr1b* and *npr3* compounds spinal phenotypes

We next asked whether *npr1b* and *npr3* work in opposition in zebrafish, as suggested by human and mouse mutant phenotypes. We generated *npr1b*$^{-/-}$*; npr3*$^{-/-}$ fish and found that adult fish still had spinal curves, most notably retaining the severe caudal spine kink seen in npr3 mutants, rather than a rescued phenotype (Figure 3). In addition, half of female *npr1b*$^{-/-}$*;npr3*$^{-/-}$ and *npr1b*$^{-/+}$*; npr3*$^{-/-}$ fish (n = 1 of 2, n = 2 of 5, respectively) had severe dwarfism. This suggests that, in zebrafish, *npr1b* and *npr3* work together to maintain spinal straightness and promote bone development.

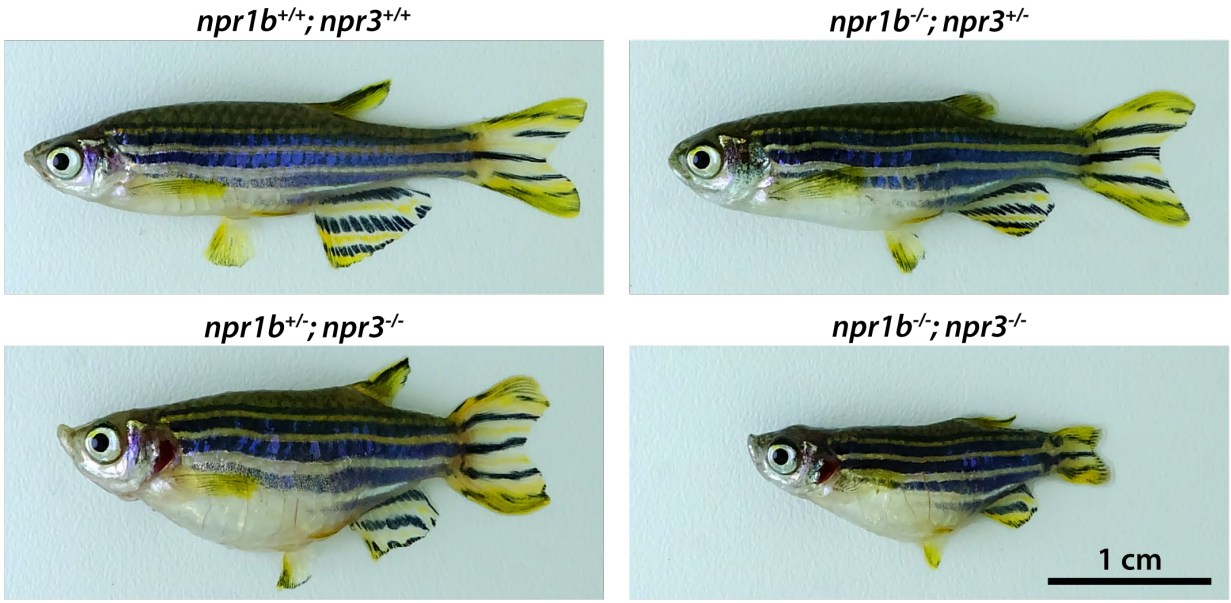


Figure 3. Combined loss of *npr1b* and *npr3* in females causes dwarfism. At 6 months of age, double mutants appear shorter than *npr1b* or *npr3* single mutants. Loss of both receptors does not rescue spinal curves. n = 2/5 female *npr1b*$^{-/-}$*;npr3*$^{-/+}$ and n = 1/2 female *npr1b*$^{-/-}$*;npr3*$^{-/-}$ fish appeared to have severe dwarfism.

Vertebral changes in *npr1b* and *npr3* mutants begin during larval development

To determine when scoliosis-like curves develop in our disease models, we performed a calcein staining time course from 7 to 15 days post fertilization (dpf) on homozygous mutants and heterozygous controls. Calcein is a fluorescent dye that binds to Ca^{2+} and is used to visualize mineralizing bone. In *npr1b* mutants, we observed a striking developmental delay in the number of calcein-stained vertebral centra in size-matched larvae (Figure 4A). This delay is most apparent at 11 dpf, or between 4-5 mm standard length (SL) (Figure 4D, F). In addition, mineralization of developing vertebral centra often appears triangular or otherwise misshapen compared to the rectangular mineralization fronts observed in heterozygous controls and by other labs (Figure 4A', arrowheads) (Bensimon-Brito et al., 2012). By 15 dpf, at approximately 6-7 mm SL, *npr1b* mutants had nearly recovered mineralized centra to WT levels (Figures 4D, F). We did not observe spinal curves in *npr1b* mutant larvae up to 15 dpf. This suggests that spinal curves in *npr1b* arise during juvenile development.

We repeated this experiment in *npr3* mutants to investigate when vertebral fusions and posterior spine curves develop. We observed that the sharp caudal spine curve in adult *npr3* mutant zebrafish first appears around 9 dpf (Figure 4B, C). As in adult fish, this curve bent to the left or right randomly and occurred in all *npr3* mutants (not shown). It appeared to develop immediately before and during the calcification process of these vertebrae (Figure 4B). *Npr3* mutants also appeared to have defects in caudal notochord flexing, which may contribute to development of these curves (Figure 4B, arrows). Unlike *npr1b* mutants, there was no change in timing of centra mineralization in *npr3* mutants (Figures 4E, G). Additionally, we did not observe any evidence through 15 dpf of vertebral fusions. This data suggests that caudal spine

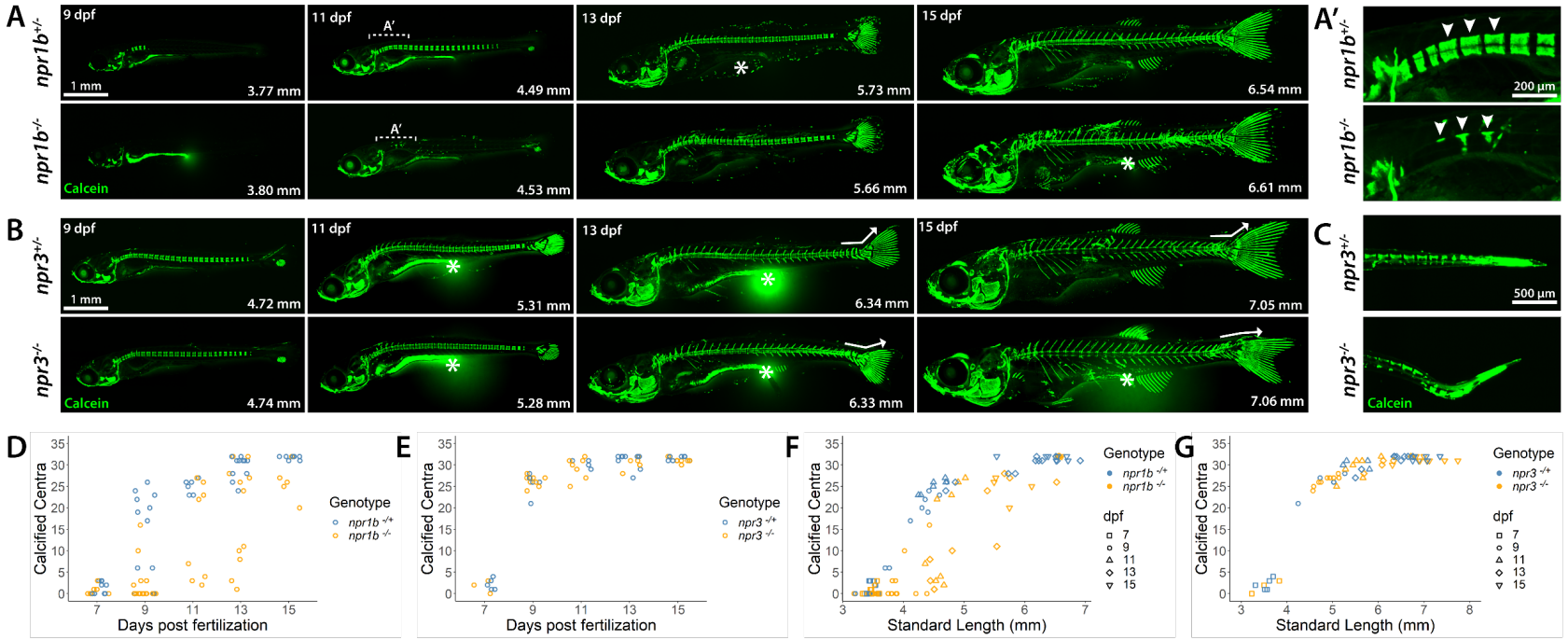


Figure 4. *Npr1b* and *npr3* are essential for proper vertebral development. *Npr1b* and *npr3* homozygous mutant larvae, along with corresponding heterozygous controls, were calcein stained and imaged at 7 (not shown), 9, 11, 13 and 15 days post-fertilization (dpf) (**A-C**). *Npr1b*$^{-/-}$ larvae had reduced vertebral calcification at 9 and 11 dpf but appeared to recover by 15 dpf (**A**). Calcification fronts in developing *npr1b*$^{-/-}$ vertebrae were shaped irregularly compared to rectangular calcification fronts in control clutchmates. Arrowheads denote vertebrae 3, 4, and 5 (**A'**). *Npr3*$^{-/-}$ larvae calcified vertebral centra normally, but develop caudal spine curves (**B**, **C**). This appears to also cause defects caudal fin ray orientation (**B**, arrows). Panel **C** shows the caudal spine curve in *npr3*$^{-/-}$ larvae from a dorsal view. *Npr1b*$^{-/-}$ fish were delayed in the number of calcein-stained centra based on both age and standard length, but appeared to rescue by 15 dpf (**D**, **F**). In comparison, npr3 mutants had no calcification delay (**E**, **G**). Standard length for each larva in A and B is noted in the bottom right corner. Asterisks (*) denote autofluorescence of gut contents and nonspecific staining skin staining, which should be ignored. Brightness/contrast levels differ for each fish shown to aid in visibility.

curves are a congenital defect in *npr3* mutants, but vertebral fusions instead occur during juvenile development.

Nppc, *npr1b*, and *npr3* are expressed in the spinal cord and notochord during vertebral development

Both *npr1b* and *npr3* are essential for spinal development around 4-5 mm SL. Previous work has described expression of *nppc* and *npr3* in CSF-cNs, but only at embryonic time points or in adult zebrafish (Prendergast et al., 2023). We used RNAScope, a fluorescent in situ hybridization method, to assess expression of *nppc*, *npr1b*, and *npr3* mRNA in 10 dpf larval sections. We observed high levels of *nppc* in a subset of spinal cord neurons adjacent to the central canal. The spacing and position of these cells matched that of CSF-contacting neurons and suggests that *nppc* is likely expressed in CSF-cNs throughout life (Figure 5E). *Nppc* and *npr3* were also expressed in the pharyngeal arches and brain (Figure 5D). *Npr1b* expression was low, but it was expressed in some CSF-cNs, in the notochord sheath and surrounding osteoblasts, and in a subset of dorsal spinal cord cells (Figure 5E). *Npr3* was expressed in putative CSF-cNs, in the notochord sheath, and was also highly expressed in the spinal cord floorplate. CSF-cNs were often triple positive for *nppc*, *npr1b*, and *npr3* (Figure 5E'). We conclude that natriuretic peptide signaling likely acts within notochord sheath cells to promote vertebral calcification.

Using CRISPR-Cas9 mutagenesis, we generated a line expressing nuclear-localized fluorescent protein Eos under control of the endogenous *nppc* promoter (*nppc:nls-Eos*). We used *nppc:nls-Eos* in combination with the *Tg[entpd5a:pkRed]*^{hu7478} reporter line (Wopat *et al.*, 2018) to assess *nppc* expression in mineralizing cell types. As with our RNAScope experiments, we identified *nppc* expression in presumptive CSF-cNs, pharyngeal arches, and brain (Figure 5A, A'). We further identified expression of *nppc* in the heart, eye, fin fold, fin rays, trunk muscle,

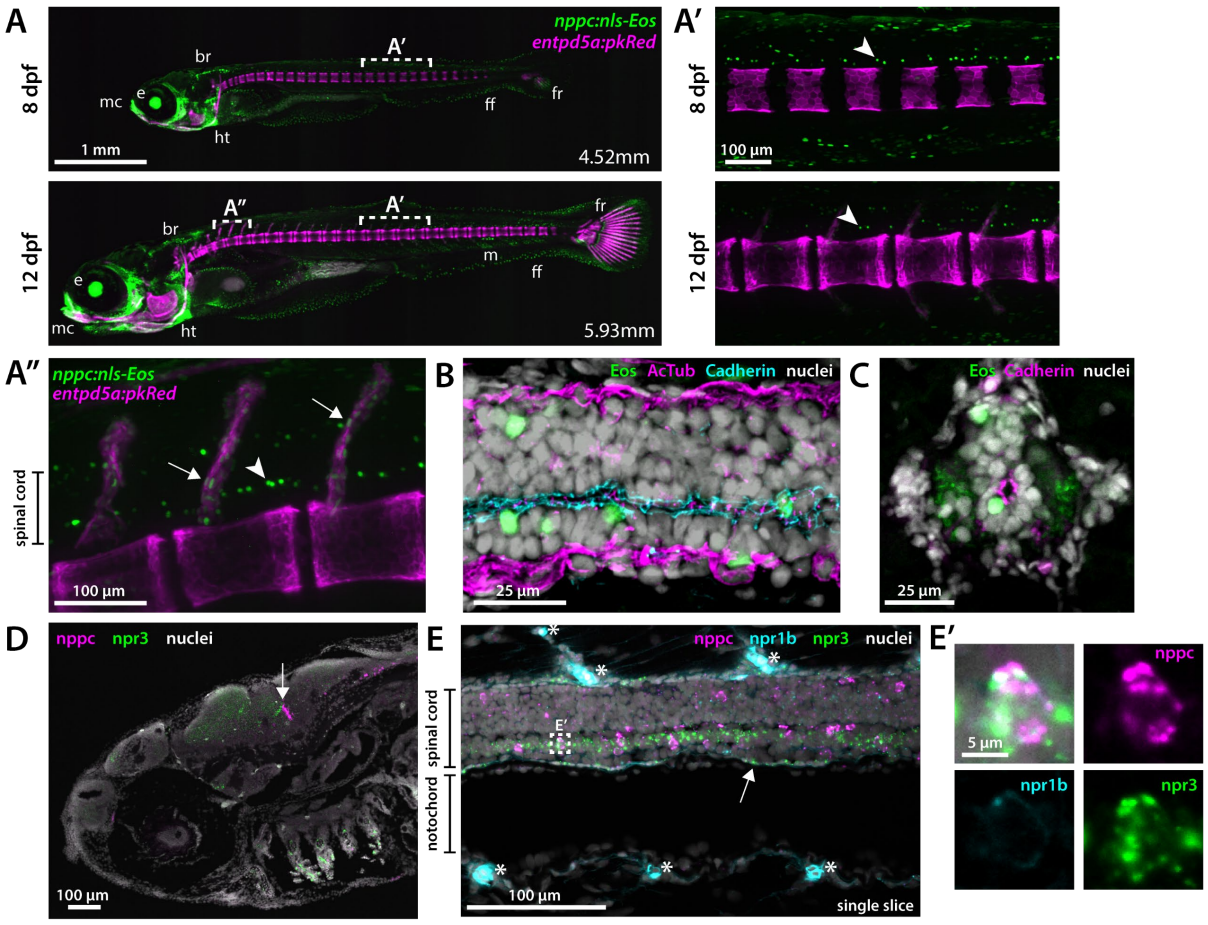


Figure 5. Natriuretic peptide pathway components are expressed within the spinal cord and notochord. *Nppc:nls-Eos* was expressed in various tissues, including the brain, heart, and spinal cord (**A**). Panels in **A'** are zooms of developing vertebrae 15-19 or 15-20 (marked by *Tg[entpd5a:pkRed]*) and adjacent Eos+ spinal cord neurons (arrowheads). At 12 dpf, Eos was also expressed in neural and haemal arch osteoblasts (arrows) (**A''**). *Nppc* expression in CSF-contacting neurons was further supported by immmunostained sections which showed Eos expression in ciliated cells adjacent to the spinal canal (**B**, sagittal section; **C**, transverse section). RNAScope expression studies confirmed this expression pattern for *nppc*. We observed expression of *npr3* as well as *nppc* in brain tissue (**D**). In addition, we observed high expression of *npr3* in the spinal cord floorplate, and lower expression of both *npr1b* and *npr3* receptors in the notochord sheath (arrow) (**E**). Asterisks indicate autofluorescence of blood vessels. Many *nppc*-high neurons also express *npr1b* and *npr3* (**E'**). AcTub, acetylated tubulin; CSF, cerebrospinal fluid; br, brain; dpf, days poststages buton; e, eye; ff, fin fold; fr, fin rays; ht, heart; m, muscle; mc, meckel's cartilage.

and craniofacial chondrocytes (including meckel's, ceratohyal, palatoquadrate, hyosymplectic, and scleral cartilages) (Figure 5A). We also observed *nppc* expression in the Weberian apparatus and in neural and haemal arches of the spine (Figure 5A''). Interestingly, *nppc:nls-Eos* appeared to turn on in arch osteoblasts just before *Tg[entpd5a:pkRed]* (not shown). *Nppc* continued to be expressed in these cell types through 6-7 mm stages (15 dpf). To examine presumed CSF-cNs in greater detail, we sectioned 10 dpf *nppc:nls-Eos* larvae and performed immunofluorescence imaging using Eos antibody. Eos+ nuclei were adjacent to the central canal and to primary cilia, further supporting expression of *nppc* in CSF-contacting neurons (Figure 5B-C). This expression pattern suggests that CSF-cNs may use CNP to translate information about spinal curves into signals that instruct other cells to modify their behavior to maintain spinal straightness.

Natriuretic Peptide signaling promotes expression of bone components

We next asked whether the delayed calcification and spinal curves we observed in npr1b and npr3 mutants are due to changes in segmentation or differentiation of notochord sheath cells. We used the *Tg[entpd5a:pkRed]* line to examine notochord sheath development in our disease models. In both *npr1b*$^{-/-}$ and *npr3*$^{-/-}$ fish, we found no changes in the number of pkRed+ notochord sheath cells or in segmentation of the notochord sheath compared to heterozygous controls (Figure 6A, B). We did *not* observe a delay in pkRed expression in npr1b mutants (Figure 6A), in contrast to our experiments assessing centra calcification (Figure 4A, D, F). We did not observe changes to pkRed+ osteoblasts in either model. However, pkRed expression intensity in notochord sheath cells was increased in *npr1b*$^{-/-}$ larvae and decreased in *npr3*$^{-/-}$ larvae, suggesting a feedback loop may act to ameliorate mineralization changes in these mutants. These results suggest that natriuretic peptide receptors act downstream of notochord

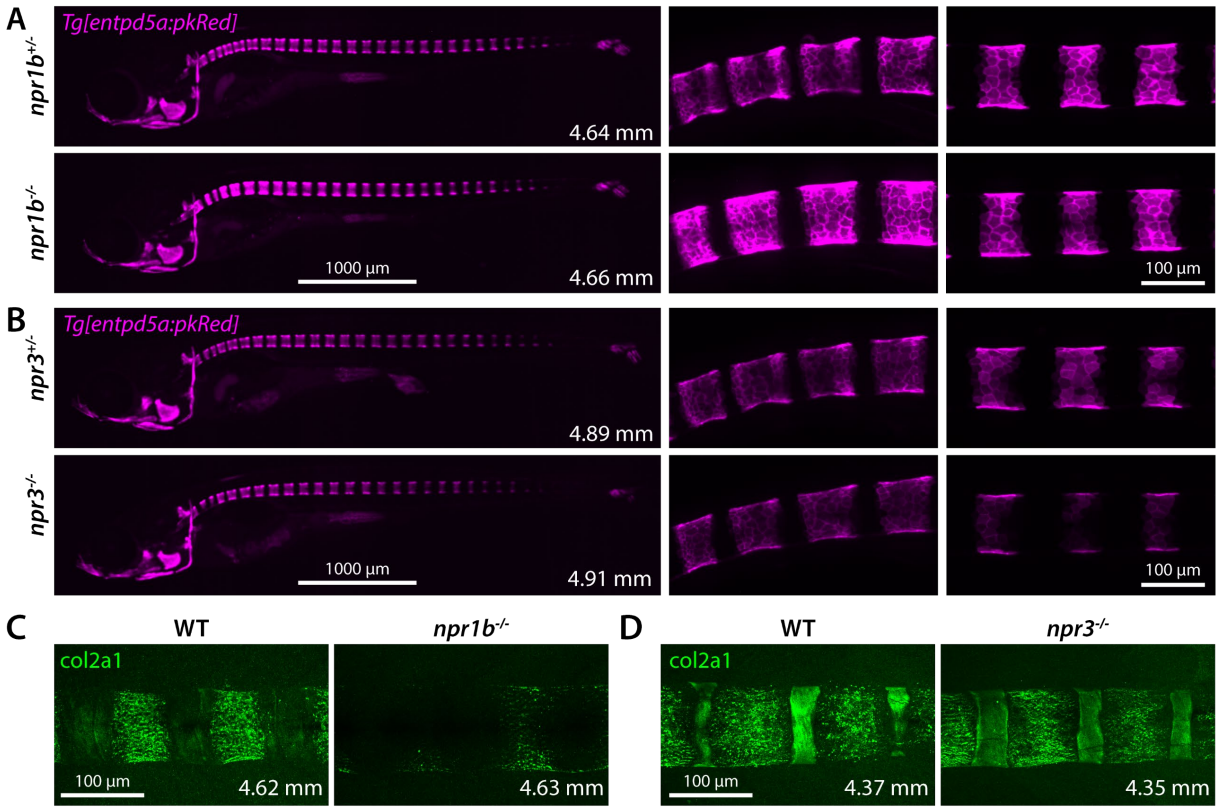


Figure 6. Natriuretic peptide receptors control expression of bone components rather than notochord segmentation. Notochord segmentation is unaffected by loss of *npr1b* or *npr3*, and the number of notochord sheath cells appeared to be unchanged. However, *Tg[entpd5a:pkRed]* expression appeared to be increased in *npr1b*$^{-/-}$ larvae and decreased in *npr3*$^{-/-}$ larvae (**A**, **B**). Middle and right panels in **A** and **B** show zooms of vertebrae 1-7 and 15-20, respectively. Loss of *npr1b* resulted in decreased collagen II (col2a1) production by the notochord sheath (**C**). Col2a1 protein levels appeared unchanged in *npr3-/-* larvae (**D**). Standard length for each larva is indicated in the bottom right.

segmentation to maintain spinal straightness, likely by controlling expression of bone matrix components.

We next assayed whether *npr1b* or *npr3* control expression of collagen by notochord sheath cells. We developed a novel protocol for whole-mount immunofluorescence of larvae

older than 5 dpf, without the need to remove skin tissue. We used this protocol to assess collagen II production by the notochord sheath in *npr1b* and *npr3* mutants. We found that *npr1b* mutant larvae had lower levels of collagen II protein in the notochord sheath compared to wild type larvae (Figure 6C). In contrast, we found no apparent difference in collagen II levels in *npr3-/-* larvae, at least at the 4.5mm stage (Figure 6D). Together, these data suggest that natriuretic peptide signaling controls expression of bone components in zebrafish.

CNP signaling is essential for maintaining spinal straightness during aging

During larval development and at adulthood, *nppc* mutants had no phenotypes other than a slight decrease in standard length (Figure 1B). However, as these fish grew older, we observed

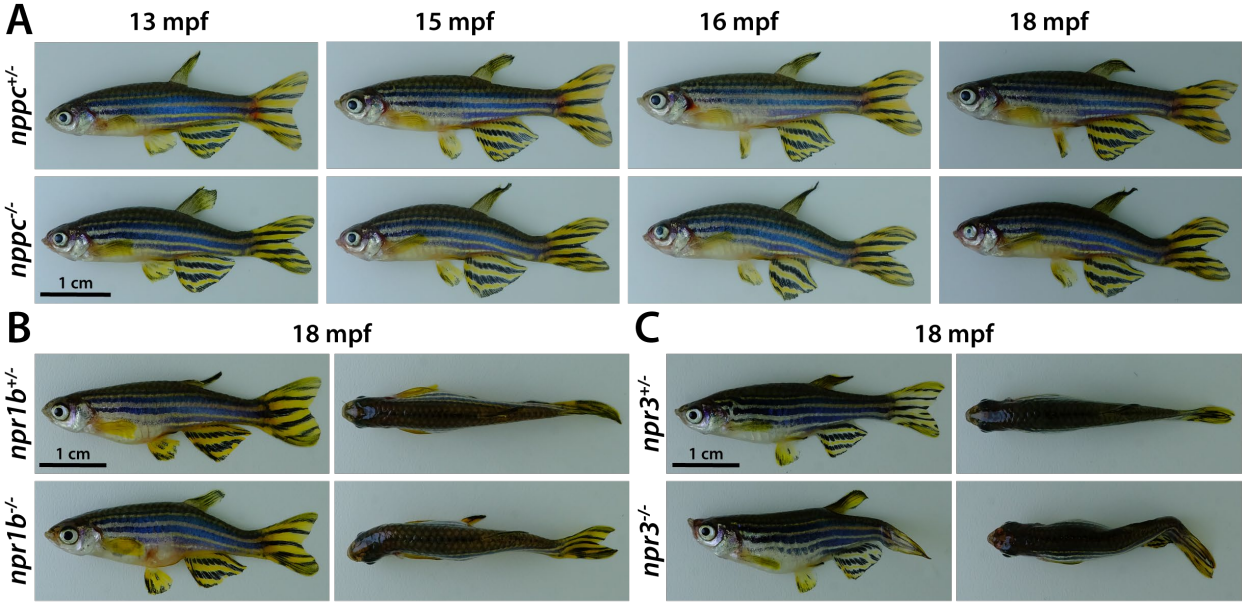


Figure 7. *Nppc* and *Npr1b* prevent aging-related kyphosis. *Nppc*$^{-/-}$ and *npr1b*$^{-/-}$ fish developed kyphosis-like curves as they aged (**A**, **B**). We tracked *nppc*$^{-/-}$ fish from 13 to 18 months post-fertilization (mpf) and found that these curves were progressive. We also noted increased rates of blindness in *nppc*$^{-/-}$ fish (**A**). The top and bottom row in **A** show the same fish over time. *Npr3*$^{-/-}$ fish did not experience accelerated aging-related kyphosis (**C**). Panels **B** and **C** include dorsal views of the same fish.

that *nppc* mutants developed aging-related kyphosis at much earlier ages than wild-type fish. To document these changes, we photographed *nppc*$^{-/-}$ and *nppc*$^{-/+}$ clutchmates monthly from 13 to 18 months post-fertilization (mpf) (Figure 7A). We observed that *nppc* homozygous mutants develop kyphosis-like curves earlier and at higher rates than heterozygous controls. These curves progressed with age. *Nppc* mutants also experienced progressive eye degeneration at higher rates than controls (see small pupil at 18 mpf in Figure 7A; lack of vision observed but not formally tested). This suggests that CNP maintains spinal straightness during aging.

We further examined aging-related kyphosis in *npr1b*$^{-/-}$ and *npr3*$^{-/-}$ fish and heterozygous controls. At 18 mpf, all *npr1b*$^{-/-}$ fish (n = 5/5) had kyphosis-like curves, compared to n = 1/13 controls (Figure 7B). The number of surviving aged *npr1b*$^{-/-}$ fish was small, but if representative, would indicate an even stronger effect than loss of *nppc*. In contrast, *npr3*$^{-/-}$ fish did not develop aging-related kyphosis (Figure 7C). This suggests that CNP signaling through Npr1b prevents aging-related kyphosis.

Discussion

Our results suggest that natriuretic peptide signaling acts throughout life to support a straight spine. Receptors Npr1b and Npr3 have distinct roles across life stages. Developmentally, Npr1b coordinates timely vertebral calcification (approx. 7 - 15 dpf) whereas Npr3 prevents caudal spine kinks. During juvenile growth (approximately 15 dpf - 3 months post fertilization), Npr1b prevents anterior spine curves while Npr3 prevents vertebral fusions. Aging reveals an additional role for natriuretic peptide signaling in maintaining a straight spine. Both *nppc* and *npr1b* prevent aging-related kyphosis, with homozygous mutants for each developing kyphosis-like curves by 18 months post-fertilization. In contrast, kyphosis is uncommon in wild type zebrafish until it markedly increases between 2-3 years of age (Hayes et al., 2013). Together, these data define stage-specific roles for natriuretic peptide signaling in establishing and then maintaining a straight spine.

Natriuretic peptide signaling likely mediates communication between the central canal of the spine and surrounding vertebral tissues across life stages. Expression of *npr1b* and *npr3* in the notochord sheath places receptor activity in mineralizing cells promoting vertebral maturation. The notochord sheath segments normally into mineralizing and intervertebral domains in *npr1b* and *npr3* mutants. In mammals, CNP signaling promotes bone growth by growth plate chondrocytes. However, we found no obvious change in the number or morphology of mineralizing notochord sheath cells and adjacent osteoblasts with *npr1b* or *npr3* loss-of-function. Instead, abnormal calcification dynamics and decreased collagen II levels in *npr1b* mutants suggest that natriuretic peptide signaling regulates bone matrix production. The later development of spinal curves in $npr1b^{-/-}$ and $npr3^{-/-}$ fish may reflect these earlier matrix and maturation changes or may reflect an entirely separate role in vertebral growth.

CNP likely acts as a signal by which cerebrospinal fluid-contacting neurons (CSF-cNs) communicate information about spine straightness to other tissues. Our expression data reinforce that CSF-cNs express *nppc*. CSF-cNs are multimodal neuropeptidergic neurons (Wyart et al., 2023), with urotensin/URP signaling exemplifying how canal-associated peptide output shapes the spine (Bearce et al., 2022; Lu et al., 2020; Zhang et al., 2018). Natriuretic peptides may be an additional peptide program operating in the same niche. In this context, *nppc* and *npr1b* expression in CSF-cNs and their mutants' aging-related kyphosis phenotypes suggest that CSF-cNs also use natriuretic peptide signaling to maintain spinal straightness throughout adulthood. Consistent with this notion, loss of *pkd2l1*, which encodes a channel necessary for CSF-cN mechanotransduction, leads to kyphosis-like curves at 12 mpf which become more severe by 19 mpf (Sternberg et al., 2018). *Nppc* also appears to be expressed in trunk muscle during larval development, and previous studies link muscle function to aging-related kyphosis. Therefore, contributions of muscle-derived CNP to kyphosis prevention should be explored further.

Npr1b and *npr3* mutants have decreased standard length in addition to spinal curves. In contrast, NPR-B and NPR-C loss-of-function have opposite phenotypes in mammals (dwarfism vs tall stature), consistent with NPR-C acting as a clearance receptor. However, lack of suppression of spinal curves in *npr1b*$^{-/-}$;*npr3*$^{-/-}$ fish suggests more complex pathway logic. Severe dwarfism in some female double mutants suggests that *npr1b* and *npr3* may instead cooperate to support vertebral growth. If so, Npr3 could act through its short cytosolic tail to inhibit adenylyl cyclase (Anand-Srivastava et al., 1990; Anand-Srivastava et al., 1996; Pagano & Anand-Srivastava, 2001), potentially combining output with Npr1b. Combined loss of NPR-A or NPR-B with NPR-C has not been studied in mammalian models. Therefore, it remains unclear whether

such an interaction is relevant to human disease or reflects differing roles of these receptors in teleosts and mammals.

The lack of spinal curves in *nppc*$^{-/-}$ fish until later adulthood complicates our understanding of natriuretic signaling and spinal straightness. A primary, unique role of *nppc* may be to maintain spinal straightness over time in adult fish. That said, other zebrafish natriuretic peptides (encoded by *nppa, nppal, nppb, nppcl,* or *nppcl2*), may redundantly signal through Npr1b and Npr3 at earlier life stages to promote vertebral maturation. Loss of *nppc* could also be buffered by compensatory expression of natriuretic peptide orthologues, with compensation becoming less effective as fish age. Further research is necessary to investigate where natriuretic peptide receptor signaling acts and how downstream signaling supports vertebral maturation and spine maintenance.

Finally, the phenotypes that develop during juvenile growth in *npr1b* and *npr3* mutants may be especially of interest for the study of Adolescent Idiopathic Scoliosis (AIS). Like in AIS, some curves in these new disease models (associated with permanently tilted heads in *npr1b* mutants, and vertebral fusions in *npr3* mutants) develop from vertebrae that appear superficially normal at earlier stages (15 dpf). Spinal curves are often more severe in female *npr1b*$^{-/-}$ or *npr3*$^{-/-}$ fish than in male siblings, consistent with the increased prevalence of AIS in females. Further research is needed to investigate whether spinal curves are consequences of early development defects (delayed mineralization in *npr1b*$^{-/-}$ larvae, and caudal spine kinks in *npr3*$^{-/-}$ fish), or whether they reflect separate roles for these receptors during juvenile growth. Regardless, these zebrafish disease models provide new tools to understand origins of spinal curves and how natriuretic peptide signaling contributes towards establishing and maintaining a straight spine.

Bridge

In the next chapter, I will discuss my work investigating whether CNP signaling has a role in regenerative fin outgrowth.

CHAPTER III. NATRIURETIC PEPTIDE SIGNALING IN FIN REGENERATION

Introduction

For decades, zebrafish have been used as a model for limb and organ regeneration. Zebrafish completely and repeatedly restore fin tissues post-injury to their original size and shape. The zebrafish caudal fin comprises 18 bony rays that taper towards the posterior end, forming the fin skeleton. This skeleton is surrounded by basal and superficial epidermis, and contains mesenchymal cells, blood vessels, and axons. The mechanisms by which regeneration of each of these tissues is precisely controlled to achieve proper fin size and shape is not fully understood. Our lab discovered that distal mesenchymal cells, or niche cells, are marked by the transcription factor Dachshund (Dach) during regeneration (Stewart et al., 2019). Dach+ cells express growth-promoting Wnts, which are essential for outgrowth (Kawakami et al., 2006). Many mesenchymal cells express Dach at 3 days post amputation (dpa), but as regeneration continues, the number of niche cells decreases, as does the rate of outgrowth (Stewart et al., 2019). As the shorter medial rays have smaller diameters and the diameter of fin rays tapers as the rays extend distally, their volume acts as a memory for the necessary outgrowth extent to restore each individual ray.

Mutants with fin overgrowth, such as *longfin*^{t2}, can be used to study the regulation of fin outgrowth. *Longfin*^{t2} is a dominant mutation causing misexpression of the potassium channel *kcnh2a* in mesenchymal cells, which causes increased Dach expression (Stewart et al., 2021). *Longfin*^{t2} animals display a regeneration speed that decreases more slowly over time than wildtype, rather than a peak regeneration speed that eclipses the wildtype (Stewart et al, 2019).

Other potassium channel mutants, or inhibition of the Ca^{2+} dependent phosphatase calcineurin, cause fins to overgrow with similar kinetics to *longfin*^{t2} (Perathoner et al., 2014; Kujawski et al., 2014). Mutations in solute carriers *slc12a7a* and *slc43a2*, which similarly affect cell membrane potential, also result in changes to fin scaling (Silic & Zhang, 2023). Our lab also discovered that loss-of-function of the voltage-gated Ca^{2+} channel *cacna1g* leads to regeneration of long fins (Le Bleu et al., 2025). Altogether, this suggests that fin scaling is controlled by membrane potential that is likely read out by voltage-gated ion channels including *cacna1g*.

C-type Natriuretic Peptide (CNP) is a candidate regulator of ion signaling. Atrial and brain natriuretic peptides regulate blood pressure, proliferation, and hypertrophy. In contrast, CNP regulates bone growth. CNP binds its receptors NPR-A or NPR-B to activate guanylyl cyclase domains and produce cyclic GMP (cGMP). The NPR-C receptor has no guanylyl cyclase domain and is thought to function as a clearance receptor, although it is also known to inhibit adenylyl cyclase (Anand-Srivastava et al., 1990; Anand-Srivastava *et* al., 1996; Cohen et al., 1996; Pagano & Anand-Srivastava, 2001). CNP overexpression, NPR2 gain-of-function, and NPR3 loss-of-function mutations cause tall stature, scoliosis, and overgrowth of digits in humans (Bocciardi et al., 2007; Boudin et al., 2018; Hannema et al., 2013; Lauffer et al., 2022; Miura et al., 2012; Miura et al., 2014; Moffatt et al., 2025). On the other hand, human NPR2 loss-of-function mutations cause dwarfism, as do NPPC loss-of-function mutations in mice (Bartels et al., 2004; Chusho et al., 2001; Hachiya et al., 2007; Khan et al., 2012; Olney et al, 2005; Sogawa et al., 2007; Tamura et al., 2004; Tsuji & Kuneida, 2005; Vasquez et al., 2013). Dwarfism due to loss of CNP in mice can be rescued by expression of CNP in growth plate chondrocytes, implying that CNP acts within bone tissue to maintain outgrowth (Chusho et al., 2001).

Many known targets of cGMP regulate ion signaling. In response to cGMP, cGMP-activated protein kinases (PKGs) phosphorylate multiple substrates resulting in decreased intracellular calcium (Francis et al., 2010). cGMP can also bind to cyclic nucleotide-gated cation channels to regulate ion flux (Biel and Michalakis, 2009). Given the role of the CNP pathway in regulation of human bone growth, its downstream regulation of calcium ion signaling, and its expression in regenerating fin tissue, this pathway could also regulate bone growth in the zebrafish fin. Thus, I hypothesized that CNP signals through Npr1/Npr2 in niche cells to inhibit Ca^{2+} fluxes and promote niche cell state.

Materials & Methods

Single-cell expression analysis

Combined 3 and 7 dpa clustering generated by our lab (Lewis et al., 2023) was used to probe expression of CNP pathway components in regenerating fins. Expression graphs were generated in R using monocle3 (Trapnell et al., 2014).

RNAScope

The RNAScope Multiplex Fluorescent kit (ACD Bio) was used to assess *nppc* expression in 3 and 7 dpa caudal fin tissue sections. We performed caudal fin amputations on wild type zebrafish and collected regenerating tissue at 3 and 7 dpa. Fin tissue was processed, embedded in paraffin blocks, and sectioned as previously described (Stewart & Stankunas, 2024). A probe was designed for *nppc* mRNA by ACD Bio. Slides were processed according to kit recommendations. Hoechst stain was used to visualize nuclei. Samples were imaged on a Zeiss LSM 880 microscope and images processed using ImageJ software.

Nppc:nls-Eos imaging – development

See chapter II for methods used to image 15 days post-fertilization (dpf) *nppc:nlsEos/+; entpd5a:pkRed/+* larvae.

Nppc:nls-Eos imaging – regeneration

See chapter II for generation of the *nppc:nls-Eos* zebrafish line. Six F_1s of the newly generated *nppc:nls-Eos* line were imaged at 3 and 7 dpa to assess expression of *nppc*. Fins were anesthetized in 0.17 g/L tricaine in fish water and amputated at the length of the principle peripheral rays using a razor blade. Fish were placed into system water to recover and monitored while breathing restarted. They were then returned to their housing tanks and allowed to regenerate until 3 dpa. At 3 dpa, they were anesthetized and placed on a microscope slide for

stitched imaging of their caudal fin. Imaging was completed within a few minutes so that fish were out of water for minimal time. Fish were placed in recovery water immediately after imaging and monitored while breathing restarted. The fish were returned to housing and allowed to regenerate until 7 dpa, when the imaging process was repeated. Images were taken using a Leica spinning disk microscope and processed using ImageJ.

Caudal fin regeneration

Adult *nppc*$^{-/-}$, *npr1b*$^{-/-}$, and *npr3*$^{-/-}$ fish and their wild type siblings (*nppc*$^{+/+}$, *npr1b*$^{+/+}$, *npr3*$^{+/+}$) were anesthetized in 0.17 g/L tricaine and imaged on a Leica spinning disk microscope to obtain photos of their caudal fins pre-amputation. These photos were also used to assess caudal fin development. Immediately after imaging, the caudal fin of each fish was amputated at the length of the principal peripheral rays using a razor blade. The fish was then placed in system water to recover and monitored while breathing restarted. At 7 and 30 dpa, regenerating caudal fins of these fish were imaged using the same process as the above section ("*Nppc:nls-Eos* imaging").

To quantify 30 dpa regenerated length, I used the segmented line tool in ImageJ to measure the distance from the amputation plane to the distal tip of fin ray 3, following dorsal-most rays after branch points. I then measured the developed distance of ray 3 using the images I took immediately pre-amputation. I matched the amputation plane in the 30 dpa image up to the pre-amputation image so that the distance measured began from the same point. This allowed me to divide the 30 dpa distance by the pre-amputation distance to obtain the proportion regenerated at 30 dpa. Significance was calculated using a two-tailed student's t test, comparing proportion regenerated for each homozygous mutant line to the proportion regenerated of their wild type siblings. Results were graphed in R software using ggplot.

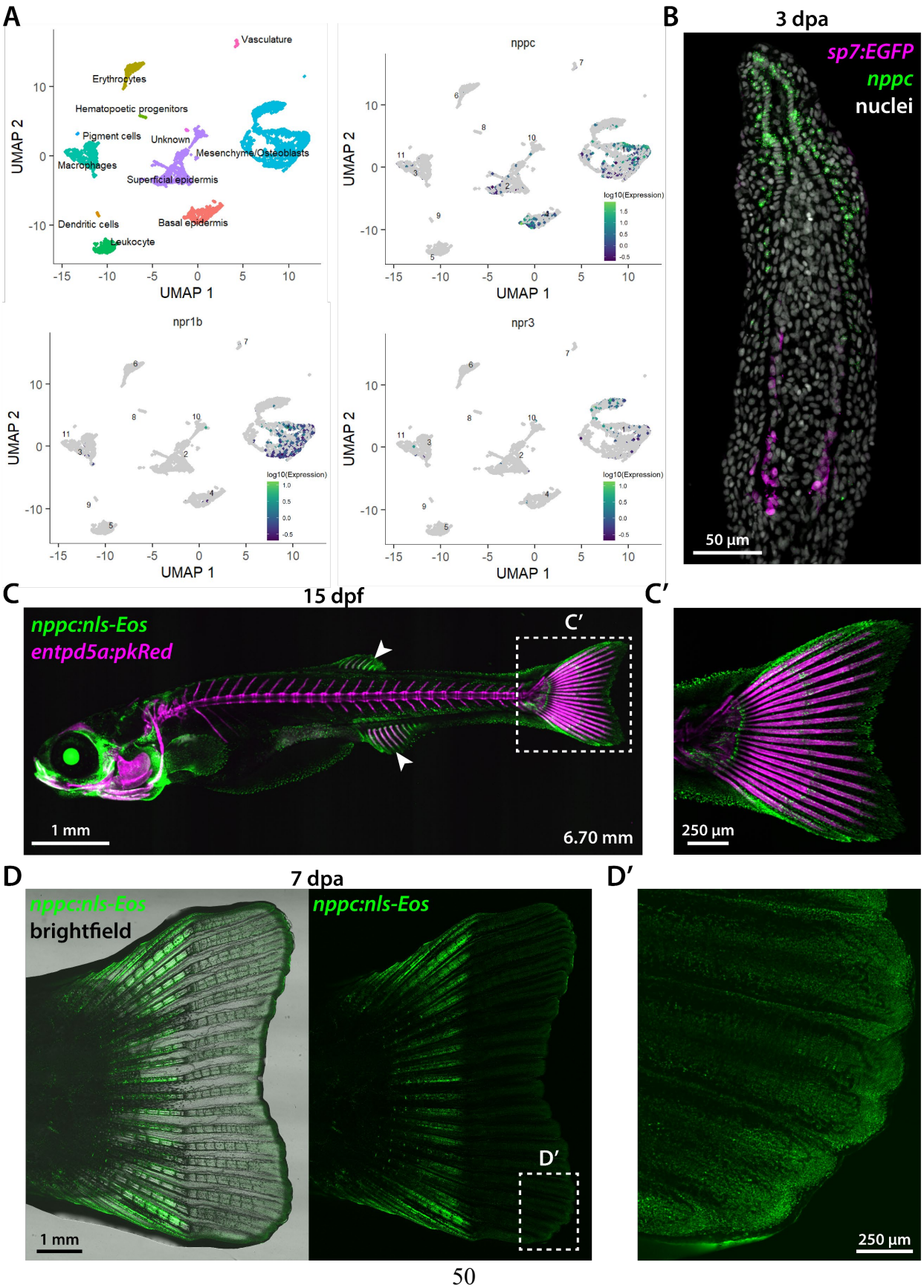
Results

CNP and its receptors are expressed in regenerating caudal fins

I first used our single-cell RNA sequencing data, generated from 3 and 7 dpa caudal fin tissue (Lewis et al., 2023), to investigate whether CNP pathway components were expressed in regenerating fins. Natriuretic peptides ANP and BNP were not expressed, but CNP (encoded by *nppc*) was expressed in regenerating fin mesenchyme and basal epidermis (Figure 8A). Natriuretic peptide receptors *npr1b* and *npr3* were also expressed in regenerating fin mesenchyme. Furthermore, *nppc* expression was concentrated in a subcluster of cells which we suspected contained the distal-most mesenchymal cells. I additionally used *nppc* RNAScope on regenerating fin sections and confirmed that *nppc* mRNA is expressed in distal mesenchyme and basal epidermis at 3 dpa (Figure 8B) and 7 dpa (not shown). These expression patterns were especially of interest to us as Wnt-producing niche cells, which we propose determine the final regenerated fin length, are located in the distal mesenchyme (Stewart et al., 2019). Therefore, we proceeded to establish zebrafish mutant lines for *nppc*, *npr1b*, and *npr3,* and the knockin reporter line *nppc:nls-Eos* (methods and non-fin phenotypes detailed in chapter II).

I used my newly generated *nppc:nls-Eos* line to investigate *nppc* expression at additional time points. During larval development, *nppc* was expressed in scattered fin fold cells as early as 48 hours post-fertilization (not shown). At 8 days post-fertilization (dpf) and 4.5 mm standard

Figure 8 (next page). CNP and its receptors are expressed in the developing and regenerating caudal fin. Single-cell RNA sequencing of 3 and 7 days post-amputation (dpa) regenerating caudal fin cells indicated that *nppc*, *npr1b,* and *npr3* were expressed in regenerating fin mesenchyme (**A**). *Nppc* was also expressed in the basal epidermis cluster. Cluster annotations are in the top left panel of **A**. 3 dpa section of a regenerating caudal fin ray, with *nppc* RNAScope in green and anti-GFP staining for *sp7:EGFP*, an osteoblast marker, in magenta (**B**). *Nppc:nls-Eos* was expressed in developing fin rays (arrowheads) and in the fin fold at 15 dpf and 6.70 mm standard length (**C**). Zoom of the caudal fin, showing increased expression around the base of developing rays, marked by *entpd5a:pkRed*+ osteoblasts (**C'**). *Nppc:nls-Eos* retained a similar expression pattern in 7 dpa adult caudal fins (**D**, **D'**)


A
Vasculature
Erythrocytes
Hematopoetic progenitors
Pigment cells
Unknown
Mesenchyme/Osteoblasts
Macrophages
Superficial epidermis
Dendritic cells
Basal epidermis
Leukocyte
UMAP 1
UMAP 2
nppc
npr1b
npr3
log10(Expression)
B
3 dpa
sp7:EGFP
nppc
nuclei
50 µm
C
15 dpf
nppc:nls-Eos
entpd5a:pkRed
C′
1 mm
6.70 mm
C′
250 µm
D
7 dpa
nppc:nls-Eos
brightfield
nppc:nls-Eos
D′
1 mm
D′
250 µm

length, I observed continued expression of *nppc* in fin fold cells (see chapter II, Figure 5A). I also observed Eos fluorescence in caudal fin rays, which were just beginning to form. At 12 dpf and 5.9 mm standard length, this expression pattern continued, with Eos fluorescence closely following osteoblast development, marked by *entpd5a:pkRed*. At 12 dpf, clusters of *nppc* expression were present which appeared to surround the base of developing caudal fin rays. In larger 15 dpf larvae and 6.70 mm standard length, I observed Eos fluorescence in developing fins rays in the pectoral (not shown), dorsal, and anal fins, suggesting that *nppc* expression in fin rays is consistent across fin types (Figure 8C [arrowheads], C'). I amputated *nppc:nls-Eos/+* adult caudal fins and found that 7 dpa regenerating caudal fins appeared to have a very similar expression pattern, with high *nppc* expression in mature fin rays and lower expression in regenerating fin tissue (Figure 8D, D'). This also matched our observations from *nppc* RNAScope experiments (Figure 8B). Combined, these developmental and regenerating expression patterns suggest that CNP signaling likely has a role in fin ray growth.

Fish lacking *npr1b* regenerate slightly shorter caudal fins

We next wondered whether loss of *nppc, npr1b,* or *npr3* affects fin development or regeneration. In adult homozygous mutants for *nppc*, *npr1b*, and *npr3*, we observed no developmental changes in fin size or structure (Figure 9A, pre-amputation images). We performed caudal fin regeneration experiments in these fish and in sibling controls by amputating the caudal fin at the tip of the principle peripheral rays and imaging the caudal fin at 7 and 30 days post-amputation (Figure 9A). Caudal fins in all three mutant lines appeared to regenerate normally – reforming rays, branching structures, and fin shape. I calculated the proportion regenerated of each caudal fin by dividing the regenerated length of ray 3 over the initial length of the ray (from amputation plane to distal tip). We identified a small but

significant decrease in percent length regenerated in *npr1b* mutant fish (Figure 9B). There were no significant regenerative changes in *nppc* or *npr3* mutant fish. This suggests that *npr1b* has a minor role in promoting fin outgrowth. Overall, despite intriguing expression patterns, natriuretic peptide signaling does not appear to be a major driver of bone growth in the regenerating caudal fin.

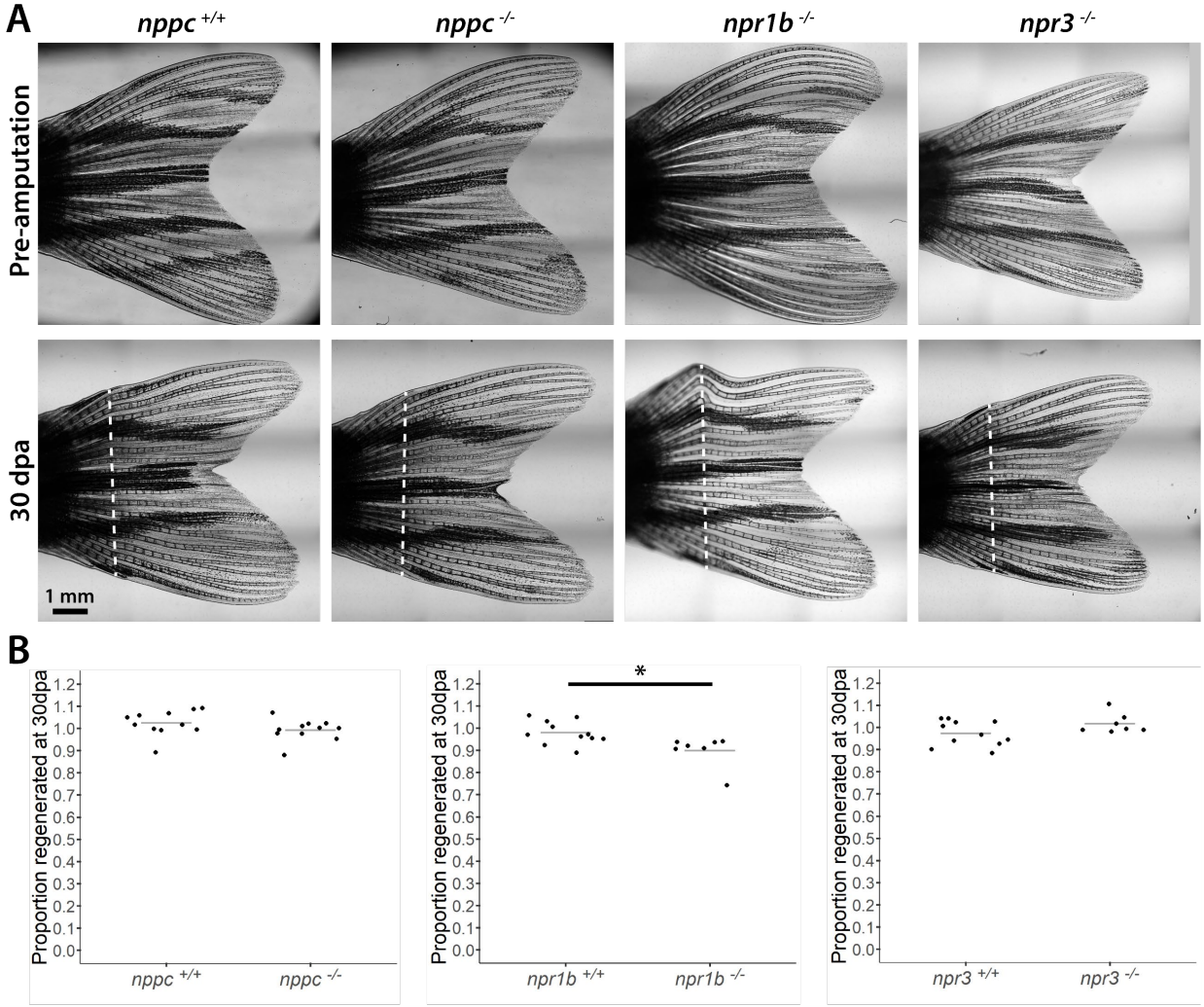


Figure 9. *Npr1b* mutants regenerate slightly shorter fins. Caudal fins developed normally in *nppc, npr1b*, and *npr3* mutants (**A**, pre-amputation images). The three mutant lines had no major defects in caudal fin regeneration (**A**, 30 dpa images). Amputation planes are marked with a dashed white line. *Npr1b*$^{-/-}$ fish regenerated slightly shorter fins compared to their original developed length (**B**). p = 0.024 (*), 2-tailed student's t-test.

Discussion

Here, I investigated the role of natriuretic peptide signaling in zebrafish caudal fin regeneration. By using our single-cell RNA sequencing dataset (Lewis et al., 2023), *nppc* RNAScope, and the *nppc:nls-Eos* reporter line that I generated, I established that *nppc* and its receptors are expressed in regenerating caudal fin tissues. Furthermore, I observed that *nppc* is expressed in developing fin rays in the pectoral, dorsal, anal, and caudal fins. I established zebrafish mutant lines for *nppc, npr1b,* and *npr3*. However, all three mutant lines appear to develop normal fins. I performed caudal fin regeneration experiments in these mutants and observed a small but significant decrease in proportional regenerated length for *npr1b* mutants. *Nppc* and *npr3* mutants had slight changes to proportional regenerated length, but these differences were not significant. Therefore, I concluded that CNP signaling likely has only a minor role in promoting bone growth during fin regeneration.

Although there were only minor regenerative changes in *npr1b* mutants, CNP signaling may still be involved in fin bone growth. In $npr1b^{-/-};npr3^{-/-}$ fish, we observed that dwarfism may worsen, suggesting that these receptors work together in zebrafish to promote bone growth (see chapter II, Figure 2). If this holds true for the caudal fin, examining fin bone growth in $npr1b^{-/-};$ $npr3^{-/-}$ double mutant fish may show a stronger effect on regeneration, or eliminate compensation by the other receptor in single mutants. In fact, especially dwarfed female $npr1b^{-/+};npr3^{-/-}$ and $npr1b^{-/-};npr3^{-/-}$ fish appeared to have smaller fins than they should for their size (bottom row of Figure 3, chapter II). Studying the double mutant phenotype, if it is consistent, is necessary to determine the role CNP signaling may play in fin outgrowth. Even if this pathway is a dead-end in terms of fin regeneration research, the *nppc:nls-Eos* line remains useful as a marker for distal

basal epidermis and mesenchyme cells, which are cell populations our lab is particularly interested in.

There are some limitations to conclusions we can draw from this work. Firstly, there are additional natriuretic peptides and receptors which may either act to compensate for loss of genes in single mutants or which may play a larger role in fin regeneration than the genes I chose to study. I chose the most highly expressed natriuretic peptide receptors based on our single-cell RNA Sequencing data, but it is possible that technical limitations resulted in transcripts for a more highly expressed peptide or receptor not being captured. Compensation by other peptides or receptors is also possible, which would explain the lack of phenotype in *nppc* mutants even though *npr1b*$^{-/-}$ fish regenerate shorter fins. Studying *npr1b*$^{-/-}$*;npr3*$^{-/-}$ double mutants will begin to address these questions. Compensation by known natriuretic peptides and receptors can also be tested in single mutants using RT-qPCR. It is also possible that CNP signaling has a larger role in promoting bone growth under conditions of environmental stress, which I did not test.

My work studying natriuretic peptide signaling has identified signaling through *npr1b* as a minor contributor to regenerative fin growth. However, there are still unanswered questions that can be addressed from this work. For instance, I only examined expression of *nppc:nls-Eos* at 3 and 7 days post-amputation. Determining whether expression of CNP remains constant throughout fin regeneration, especially through photoconversion of Eos fluorescent protein, or whether it is expressed more highly at early or late stages of regeneration could narrow down time points to investigate more closely. As I mentioned above, examining fin regeneration in double mutants or performing quantitative PCR could help determine whether compensation masks the role of CNP signaling in single mutants. And even though *npr1b* mutants only have a minor regenerative phenotype, studying this model would still improve our understanding of fin

regeneration and the multiple pathways which act to ensure the regeneration of properly scaled fins. I look forward to seeing how these mutant lines will be used in the future!

Bridge

In the next chapter, I will provide a summary of the results and significance of the work described in this chapter and in chapter II. I will also discuss future avenues of research to be pursued following this dissertation.

CHAPTER IV. CONCLUDING SUMMARY

Summary

In this dissertation, I investigated potential roles of C-type Natriuretic Peptide signaling in fin regeneration and spinal development and maintenance. We began this project by reviewing the literature and observing that CNP signaling is involved in the regulation of bone length in mammals. Therefore, it may be also involved in zebrafish fin bone scaling. I established four zebrafish lines which will continue to be of use to the scientific community: *nppc*$^{-/-}$, *npr1b*$^{-/-}$, *npr3*$^{-/-}$, and *nppc:nls-Eos*. I examined adult mutants for *nppc, npr1b,* and *npr3* and found that although no mutants had fin development phenotypes, *npr1b* and *npr3* mutants developed spinal curves. I found that *npr1b* and *npr3* were required at multiple time points – both during initial vertebral calcification and during juvenile growth – for the development of a straight spine. Furthermore, both *nppc* and *npr1b* were required to prevent the early development of kyphosis-like curves, suggesting that they either act to maintain spinal straightness or that they have an aging-specific role. *Nppc*, *npr1b*, and *npr3* appeared to be expressed in CSF-contacting neurons (CSF-cNs), which are known to have a role in developing and maintaining spinal straightness. This begins to explain how CNP signaling is important for not just bone scaling, but also *straightness* of the spine. For instance, CSF-cNs, which can detect spinal curvatures, may increase CNP signaling on the concave side when curvature is detected, increasing bone growth to straighten out the curve. Future research is needed to elucidate the function of CSF-cNs and to determine how they communicate curves to other cell types.

I also determined that single mutants for *nppc, npr1b* and *npr3* did not majorly affect fin regeneration or development. *Npr1b*$^{-/-}$ fish had only a minor decrease in regenerated length.

However, more work would be needed to rule out natriuretic peptide signaling as a promoter of bone growth in zebrafish fins. Double *npr1b*$^{-/-}$;*npr3*$^{-/-}$ mutant fish, which occasionally have short fins, suggest that compensation by other natriuretic peptides or receptors may have masked phenotypes in single mutants. Although these mutants had only minor fin regeneration phenotypes, my work studying spinal development and maintenance in these mutants will be of great use to the spinal development field.

Unanswered Questions

My work leaves open many new questions to explore. In terms of vertebral development, the ideal next step would be to verify that CNP signaling promotes expression of bone components. This could be done through RNA sequencing of *npr1b* and *npr3* mutants. My work also suggests that CNP signaling acts within notochord sheath cells to promote vertebral development. Generating conditional mutant lines that lack these receptors in the notochord sheath but not surrounding tissues, for example by expressing Cas9 under the *entpd5a* promoter and constitutively expressing the guide RNAs I used here, would help answer this question. It would also be interesting to attempt to rescue loss of *npr1b* or *npr3* at early stages in these mutants, perhaps by expressing the receptors under a heat shock promoter, and test whether spinal curves that develop during juvenile growth in these mutants are secondary to early effects on the spine (such as delayed mineralization), or whether they represent separate and ongoing contributions of these receptors to vertebral growth.

Another question raised by my work, and which is also brought up by the study of Urp neuropeptides (Bearce et al., 2022), is how small peptides expressed by CSF-cNs can exert effects outside of the spinal cord. The conventional view is that CSF-cNs secrete peptides into the cerebrospinal fluid of the central canal. However, my results here and the Urp literature suggest that these peptides exit the spinal cord to signal to other cell types. Perhaps CSF-cNs have axons which exit the spinal cord, through which CSF-cNs secrete peptides targeted towards surrounding tissues. Another possibility is that these small peptides diffuse or are trafficked out of the spinal cord into adjacent tissues or the bloodstream. High expression of *npr3* in floorplate neurons could represent a function regulating the amount of CNP which diffuses out of the spinal

cord. It is essential to explore this question so that we can fully understand how CSF-cNs communicate to other cell types to maintain a straight spine.

In terms of fin regeneration, I discussed experiments in chapter III which would help determine whether natriuretic peptide signaling regulates fin bone developmental or regeneration. I recommend starting by investigating the short fin phenotype I observed in one female out of the 4 *npr1b*$^{-/-}$;*npr3*$^{-/-}$ double mutants I was able to generate. It is important to establish whether this phenotype is consistent by breeding more double mutants and examining their development. The length of fins in these mutants should also be measured and compared to wild type fish of similar standard length, to determine whether these fins are merely a result of dwarfism in these fish or whether they reflect a separate role for natriuretic peptide receptors in fin development. Then, fin amputations and imaging must be performed to determine whether these double mutants have a regeneration-specific phenotype. The other RNAScope probes for *npr1b* and *npr3* can also be used to determine which cell populations express these receptors, if the mutants I generated continue to be of interest to the lab.

In this work, I chose to generate zebrafish mutants for *npr1b* rather than *npr2*, which is the receptor implicated by human phenotypes. It would be interesting to generate zebrafish mutants for *npr2* and test whether this receptor is also involved in vertebral growth or fin regeneration. It would also be worth testing whether compensation by another natriuretic peptide in *nppc* mutants masks earlier effects in this mutant, or whether CNP is simply more important for maintaining the spine during the aging process. This could be done by performing quantitative RT-PCR for the other natriuretic peptide genes (listed in the Discussion section, chapter II) and receptors using spine or caudal fin tissue. These are only a few examples of new questions generated by this work that merit further study.

Concluding Thoughts

Spinal curves can be caused by a myriad of disorders. In this dissertation, I investigated how perturbations in CNP signaling cause spinal curves. The zebrafish lines I generated will be a useful tool to continue investigating the role of CNP in vertebral growth and maintenance, and potentially in fin development and regeneration. Studying these mutants may even lead to new therapies for scoliosis or dwarfism caused by deficient CNP signaling. Furthermore, my work reveals that CNP signaling acts across life stages in zebrafish to maintain a straight spine. This is especially of interest for the study of idiopathic scoliosis, as curves develop during juvenile growth in *npr1b* and *npr3* mutants from vertebrae that appear overtly normal at earlier stages. Expression of CNP and its receptors in CSF-cNs, and the fact that *pkd2l1* mutants develop extremely similar kyphosis-like curves to *nppc* mutants, also supports the theory that CSF-cNs may use CNP to maintain straightness throughout life. Studying these mutants advances our understanding of normal vertebral development and the signaling-regulated processes that keep the spine straight.

REFERENCES CITED

Anand-Srivastava, M. B., Sairam, M. R., & Cantin, M. (1990). Ring-deleted analogs of atrial natriuretic factor inhibit adenylate cyclase/cAMP system. Possible coupling of clearance atrial natriuretic factor receptors to adenylate cyclase/cAMP signal transduction system. *The Journal of biological chemistry, 265*(15), 8566–8572.

Anand-Srivastava, M. B., Sehl, P. D., & Lowe, D. G. (1996). Cytoplasmic domain of natriuretic peptide receptor-C inhibits adenylyl cyclase. Involvement of a pertussis toxin-sensitive G protein. *The Journal of biological chemistry, 271*(32), 19324–19329. https://doi.org/10.1074/jbc.271.32.19324

Bearce, E. A., Irons, Z. H., O'Hara-Smith, J. R., Kuhns, C. J., Fisher, S. I., Crow, W. E., & Grimes, D. T. (2022). Urotensin II-related peptides, Urp1 and Urp2, control zebrafish spine morphology. *eLife*, *11*, e83883. https://doi.org/10.7554/eLife.83883

Bartels, C. F., Bükülmez, H., Padayatti, P., Rhee, D. K., van Ravenswaaij-Arts, C., Pauli, R. M., Mundlos, S., Chitayat, D., Shih, L. Y., Al-Gazali, L. I., Kant, S., Cole, T., Morton, J., Cormier-Daire, V., Faivre, L., Lees, M., Kirk, J., Mortier, G. R., Leroy, J., Zabel, B., … Warman, M. L. (2004). Mutations in the transmembrane natriuretic peptide receptor NPR-B impair skeletal growth and cause acromesomelic dysplasia, type Maroteaux. *American journal of human genetics, 75*(1), 27–34. https://doi.org/10.1086/422013

Bensimon-Brito, A., Cardeira, J., Cancela, M. L., Huysseune, A., & Witten, P. E. (2012). Distinct patterns of notochord mineralization in zebrafish coincide with the localization of Osteocalcin isoform 1 during early vertebral centra formation. *BMC developmental biology, 12,* 28. https://doi.org/10.1186/1471-213X-12-28

Bhattacharya, D., & Van Meir, E. G. (2019). A simple genotyping method to detect small CRISPR-Cas9 induced indels by agarose gel electrophoresis. *Scientific reports, 9*(1), 4437. https://doi.org/10.1038/s41598-019-39950-4

Biel, M., & Michalakis, S. (2009). Cyclic nucleotide-gated channels. *Handbook of experimental pharmacology*, (191), 111–136. https://doi.org/10.1007/978-3-540-68964-5_7

Bocciardi, R., Giorda, R., Buttgereit, J., Gimelli, S., Divizia, M. T., Beri, S., Garofalo, S., Tavella, S., Lerone, M., Zuffardi, O., Bader, M., Ravazzolo, R., & Gimelli, G. (2007). Overexpression of the C-type natriuretic peptide (CNP) is associated with overgrowth and bone anomalies in an individual with balanced t(2;7) translocation. *Human mutation, 28*(7), 724–731. https://doi.org/10.1002/humu.20511

Boudin, E., de Jong, T. R., Prickett, T., Lapauw, B., Toye, K., Van Hoof, V., Luyckx, I., Verstraeten, A., Heymans, H., Dulfer, E., Van Laer, L., Berry, I. R., Dobbie, A., Blair, E., Loeys, B., Espiner, E. A., Wit, J. M., Van Hul, W., Houpt, P., & Mortier, G. R. (2018). Bi-allelic Loss-of-Function Mutations in the NPR-C Receptor Result in Enhanced Growth and Connective Tissue Abnormalities. *American journal of human genetics, 103*(2), 288–295. https://doi.org/10.1016/j.ajhg.2018.06.007

Chusho, H., Tamura, N., Ogawa, Y., Yasoda, A., Suda, M., Miyazawa, T., Nakamura, K., Nakao, K., Kurihara, T., Komatsu, Y., Itoh, H., Tanaka, K., Saito, Y., Katsuki, M., & Nakao, K. (2001). Dwarfism and early death in mice lacking C-type natriuretic peptide. *Proceedings of the National Academy of Sciences of the United States of America, 98*(7), 4016–4021. https://doi.org/10.1073/pnas.071389098

Cohen, D., Koh, G. Y., Nikonova, L. N., Porter, J. G., & Maack, T. (1996). Molecular determinants of the clearance function of type C receptors of natriuretic peptides. *The Journal of biological chemistry, 271*(16), 9863–9869. https://doi.org/10.1074/jbc.271.16.9863

Dauphinee, S. M., Eva, M. M., Yuki, K. E., Herman, M., Vidal, S. M., & Malo, D. (2013). Characterization of two ENU-induced mutations affecting mouse skeletal morphology. *G3 (Bethesda, Md.), 3*(10), 1753–1758. https://doi.org/10.1534/g3.113.007310

Esapa, C. T., Piret, S. E., Nesbit, M. A., Loh, N. Y., Thomas, G., Croucher, P. I., Brown, M. A., Brown, S. D., Cox, R. D., & Thakker, R. V. (2016). Mice with an N-Ethyl-N-Nitrosourea (ENU) Induced Tyr209Asn Mutation in Natriuretic Peptide Receptor 3 (NPR3) Provide a Model for Kyphosis Associated with Activation of the MAPK Signaling Pathway. *PloS one, 11*(12), e0167916. https://doi.org/10.1371/journal.pone.0167916

Francis, S. H., Busch, J. L., Corbin, J. D., & Sibley, D. (2010). cGMP-dependent protein kinases and cGMP phosphodiesterases in nitric oxide and cGMP action. *Pharmacological reviews, 62*(3), 525–563. https://doi.org/10.1124/pr.110.002907

Grimes Lab. (n.d.). *Calcein staining of Zebrafish Larvae*. https://static1.squarespace.com/static/5b32df0ea2772c8721146b7f/t/5f1b7cb8e3ddcd47257e910a/1595636920592/Calcein+staining+of+zebrafish+larvae.pdf

Hachiya, R., Ohashi, Y., Kamei, Y., Suganami, T., Mochizuki, H., Mitsui, N., Saitoh, M., Sakuragi, M., Nishimura, G., Ohashi, H., Hasegawa, T., & Ogawa, Y. (2007). Intact kinase homology domain of natriuretic peptide receptor-B is essential for skeletal development. *The Journal of clinical endocrinology and metabolism, 92*(10), 4009–4014. https://doi.org/10.1210/jc.2007-1101

Hannema, S. E., van Duyvenvoorde, H. A., Premsler, T., Yang, R. B., Mueller, T. D., Gassner, B., Oberwinkler, H., Roelfsema, F., Santen, G. W., Prickett, T., Kant, S. G., Verkerk, A. J., Uitterlinden, A. G., Espiner, E., Ruivenkamp, C. A., Oostdijk, W., Pereira, A. M., Losekoot, M., Kuhn, M., & Wit, J. M. (2013). An activating mutation in the kinase homology domain of the natriuretic peptide receptor-2 causes extremely tall stature without skeletal deformities. *The Journal of clinical endocrinology and metabolism, 98*(12), E1988–E1998. https://doi.org/10.1210/jc.2013-2358

Hayes, A. J., Reynolds, S., Nowell, M. A., Meakin, L. B., Habicher, J., Ledin, J., Bashford, A., Caterson, B., & Hammond, C. L. (2013). Spinal deformity in aged zebrafish is accompanied by degenerative changes to their vertebrae that resemble osteoarthritis. *PloS one*, *8*(9), e75787. https://doi.org/10.1371/journal.pone.0075787

Jaubert, J., Jaubert, F., Martin, N., Washburn, L. L., Lee, B. K., Eicher, E. M., & Guénet, J. L. (1999). Three new allelic mouse mutations that cause skeletal overgrowth involve the natriuretic peptide receptor C gene (Npr3). *Proceedings of the National Academy of Sciences of the United States of America, 96*(18), 10278–10283. https://doi.org/10.1073/pnas.96.18.10278

Kawakami, Y., Rodriguez Esteban, C., Raya, M., Kawakami, H., Martí, M., Dubova, I., & Izpisúa Belmonte, J. C. (2006). Wnt/beta-catenin signaling regulates vertebrate limb regeneration. *Genes & development, 20*(23), 3232–3237. https://doi.org/10.1101/gad.1475106

Khan, S., Ali, R. H., Abbasi, S., Nawaz, M., Muhammad, N., & Ahmad, W. (2012). Novel mutations in natriuretic peptide receptor-2 gene underlie acromesomelic dysplasia, type maroteaux. *BMC medical genetics, 13*, 44. https://doi.org/10.1186/1471-2350-13-44

Kujawski, S., Lin, W., Kitte, F., Börmel, M., Fuchs, S., Arulmozhivarman, G., Vogt, S., Theil, D., Zhang, Y., & Antos, C. L. (2014). Calcineurin regulates coordinated outgrowth of zebrafish regenerating fins. *Developmental cell*, *28*(5), 573–587. https://doi.org/10.1016/j.devcel.2014.01.019

Labun, K., Montague, T. G., Krause, M., Torres Cleuren, Y. N., Tjeldnes, H., & Valen, E. (2019). CHOPCHOP v3: expanding the CRISPR web toolbox beyond genome editing. *Nucleic acids research*, *47*(W1), W171–W174. https://doi.org/10.1093/nar/gkz365

Lauffer, P., Boudin, E., van der Kaay, D. C. M., Koene, S., van Haeringen, A., van Tellingen, V., Van Hul, W., Prickett, T. C. R., Mortier, G., Espiner, E. A., & van Duyvenvoorde, H. A. (2022). Broadening the Spectrum of Loss-of-Function Variants in NPR-C-Related Extreme Tall Stature. *Journal of the Endocrine Society, 6*(4), bvac019. https://doi.org/10.1210/jendso/bvac019

Lawrence, C., & Mason, T. (2012). Zebrafish housing systems: a review of basic operating principles and considerations for design and functionality. *ILAR journal*, *53*(2), 179–191. https://doi.org/10.1093/ilar.53.2.179

Le Bleu, H. K., Kioussi, R. G., Henner, A. L., Lewis, V. M., Stewart, S., & Stankunas, K. (2025). Voltage-gated calcium channels generate blastema Ca2+ fluxes restraining zebrafish fin regenerative outgrowth. *Development (Cambridge, England)*, *152*(23), dev204739. https://doi.org/10.1242/dev.204739

Lewis, V. M., Le Bleu, H. K., Henner, A. L., Markovic, H., Robbins, A. E., Stewart, S., & Stankunas, K. (2023). Insulin-like growth factor receptor / mTOR signaling elevates global translation to accelerate zebrafish fin regenerative outgrowth. *Developmental biology*, *502*, 1–13. https://doi.org/10.1016/j.ydbio.2023.05.008

Lu, H., Shagirova, A., Goggi, J. L., Yeo, H. L., & Roy, S. (2020). Reissner fibre-induced urotensin signalling from cerebrospinal fluid-contacting neurons prevents scoliosis of the vertebrate spine. *Biology open*, *9*(5), bio052027. https://doi.org/10.1242/bio.052027

Matsukawa, N., Grzesik, W. J., Takahashi, N., Pandey, K. N., Pang, S., Yamauchi, M., & Smithies, O. (1999). The natriuretic peptide clearance receptor locally modulates the physiological effects of the natriuretic peptide system. *Proceedings of the National Academy of Sciences of the United States of America, 96*(13), 7403–7408. https://doi.org/10.1073/pnas.96.13.7403

Miura, K., Kim, O. H., Lee, H. R., Namba, N., Michigami, T., Yoo, W. J., Choi, I. H., Ozono, K., & Cho, T. J. (2014). Overgrowth syndrome associated with a gain-of-function mutation of the natriuretic peptide receptor 2 (NPR2) gene. *American journal of medical genetics. Part A, 164A*(1), 156–163. https://doi.org/10.1002/ajmg.a.36218

Miura, K., Namba, N., Fujiwara, M., Ohata, Y., Ishida, H., Kitaoka, T., Kubota, T., Hirai, H., Higuchi, C., Tsumaki, N., Yoshikawa, H., Sakai, N., Michigami, T., & Ozono, K. (2012). An overgrowth disorder associated with excessive production of cGMP due to a gain-of-function mutation of the natriuretic peptide receptor 2 gene. *PloS one, 7*(8), e42180. https://doi.org/10.1371/journal.pone.0042180

Moffatt, P., Janelle, C., Miranda, V., Bardai, G., & Rauch, F. (2025). Tall Stature and Scoliosis Associated With a Novel Homozygous Loss-of-Function Missense Variant in NPR3. *American journal of medical genetics. Part A*, *197*(8), e64080. https://doi.org/10.1002/ajmg.a.64080

Olney, R. C., Bükülmez, H., Bartels, C. F., Prickett, T. C., Espiner, E. A., Potter, L. R., & Warman, M. L. (2006). Heterozygous mutations in natriuretic peptide receptor-B (NPR2) are associated with short stature. *The Journal of clinical endocrinology and metabolism, 91*(4), 1229–1232. https://doi.org/10.1210/jc.2005-1949

Pagano, M., & Anand-Srivastava, M. B. (2001). Cytoplasmic domain of natriuretic peptide receptor C constitutes Gi activator sequences that inhibit adenylyl cyclase activity. *The Journal of biological chemistry, 276*(25), 22064–22070. https://doi.org/10.1074/jbc.M101587200

Perathoner, S., Daane, J. M., Henrion, U., Seebohm, G., Higdon, C. W., Johnson, S. L., Nüsslein-Volhard, C., & Harris, M. P. (2014). Bioelectric signaling regulates size in zebrafish fins. *PLoS genetics, 10*(1), e1004080. https://doi.org/10.1371/journal.pgen.1004080

Prendergast, A. E., Jim, K. K., Marnas, H., Desban, L., Quan, F. B., Djenoune, L., Laghi, V., Hocquemiller, A., Lunsford, E. T., Roussel, J., Keiser, L., Lejeune, F. X., Dhanasekar, M., Bardet, P. L., Levraud, J. P., van de Beek, D., Vandenbroucke-Grauls, C. M. J. E., & Wyart, C. (2023). CSF-contacting neurons respond to Streptococcus pneumoniae and promote host survival during central nervous system infection. *Current biology : CB, 33*(5), 940–956.e10. https://doi.org/10.1016/j.cub.2023.01.039

Silic, M. R., & Zhang, G. (2023). Bioelectricity in Developmental Patterning and Size Control: Evidence and Genetically Encoded Tools in the Zebrafish Model. *Cells*, *12*(8), 1148. https://doi.org/10.3390/cells12081148

Sogawa, C., Tsuji, T., Shinkai, Y., Katayama, K., & Kunieda, T. (2007). Short-limbed dwarfism: slw is a new allele of Npr2 causing chondrodysplasia. *The Journal of heredity, 98*(6), 575–580. https://doi.org/10.1093/jhered/esm065

Stewart, S., Le Bleu, H. K., Yette, G. A., Henner, A. L., Robbins, A. E., Braunstein, J. A., & Stankunas, K. (2021). longfin causes cis-ectopic expression of the kcnh2a ether-a-go-go K+ channel to autonomously prolong fin outgrowth. *Development (Cambridge, England)*, *148*(11), dev199384. https://doi.org/10.1242/dev.199384

Stewart, S., & Stankunas, K. (2024). Section Immunostaining for Protein Expression and Cell Proliferation Studies of Regenerating Fins. *Methods in molecular biology (Clifton, N.J.)*, *2707*, 235–254. https://doi.org/10.1007/978-1-0716-3401-1_16

Stewart, S., Yette, G. A., Le Bleu, H. K., Henner, A. L., Braunstein, J. A., Chehab, J. W., Harms, M. J., & Stankunas, K. (2019). Skeletal geometry and niche transitions restore organ size and shape during zebrafish fin regeneration. *bioRxiv 606970*. https://doi.org/10.1101/606970

Sternberg, J. R., Prendergast, A. E., Brosse, L., Cantaut-Belarif, Y., Thouvenin, O., Orts-Del'Immagine, A., Castillo, L., Djenoune, L., Kurisu, S., McDearmid, J. R., Bardet, P. L., Boccara, C., Okamoto, H., Delmas, P., & Wyart, C. (2018). Pkd2l1 is required for mechanoception in cerebrospinal fluid-contacting neurons and maintenance of spine curvature. *Nature communications, 9*(1), 3804. https://doi.org/10.1038/s41467-018-06225-x

Suda, M., Ogawa, Y., Tanaka, K., Tamura, N., Yasoda, A., Takigawa, T., Uehira, M., Nishimoto, H., Itoh, H., Saito, Y., Shiota, K., & Nakao, K. (1998). Skeletal overgrowth in transgenic mice that overexpress brain natriuretic peptide. *Proceedings of the National Academy of Sciences of the United States of America, 95*(5), 2337–2342. https://doi.org/10.1073/pnas.95.5.2337

Suga, S., Nakao, K., Hosoda, K., Mukoyama, M., Ogawa, Y., Shirakami, G., Arai, H., Saito, Y., Kambayashi, Y., & Inouye, K. (1992). Receptor selectivity of natriuretic peptide family, atrial natriuretic peptide, brain natriuretic peptide, and C-type natriuretic peptide. *Endocrinology, 130*(1), 229–239. https://doi.org/10.1210/endo.130.1.1309330

Tamura, N., Doolittle, L. K., Hammer, R. E., Shelton, J. M., Richardson, J. A., & Garbers, D. L. (2004). Critical roles of the guanylyl cyclase B receptor in endochondral ossification and development of female reproductive organs. *Proceedings of the National Academy of Sciences of the United States of America, 101*(49), 17300–17305. https://doi.org/10.1073/pnas.0407894101

Thisse, B., & Thisse, C. (n.d.). *Protocol for In Situ Hybridization on whole mount zebrafish embryos*. ZFIN The Zebrafish Information Network. https://zfin.org/ZFIN/Methods/ThisseProtocol.html

Trapnell, C., Cacchiarelli, D., Grimsby, J., Pokharel, P., Li, S., Morse, M., Lennon, N. J., Livak, K. J., Mikkelsen, T. S., & Rinn, J. L. (2014). The dynamics and regulators of cell fate decisions are revealed by pseudotemporal ordering of single cells. *Nature biotechnology*, *32*(4), 381–386. https://doi.org/10.1038/nbt.2859

Tsuji, T., & Kunieda, T. (2005). A loss-of-function mutation in natriuretic peptide receptor 2 (Npr2) gene is responsible for disproportionate dwarfism in cn/cn mouse. *The Journal of biological chemistry, 280*(14), 14288–14292. https://doi.org/10.1074/jbc.C500024200

Vasques, G. A., Amano, N., Docko, A. J., Funari, M. F., Quedas, E. P., Nishi, M. Y., Arnhold, I. J., Hasegawa, T., & Jorge, A. A. (2013). Heterozygous mutations in natriuretic peptide receptor-B (NPR2) gene as a cause of short stature in patients initially classified as idiopathic short stature. *The Journal of clinical endocrinology and metabolism, 98*(10), E1636–E1644. https://doi.org/10.1210/jc.2013-2142

Walker, M. B., & Kimmel, C. B. (2007). A two-color acid-free cartilage and bone stain for zebrafish larvae. *Biotechnic & histochemistry : official publication of the Biological Stain Commission*, *82*(1), 23–28. https://doi.org/10.1080/10520290701333558

Wopat, S., Bagwell, J., Sumigray, K. D., Dickson, A. L., Huitema, L. F. A., Poss, K. D., Schulte-Merker, S., & Bagnat, M. (2018). Spine Patterning Is Guided by Segmentation of the Notochord Sheath. *Cell reports, 22*(8), 2026–2038. https://doi.org/10.1016/j.celrep.2018.01.084

Wyart C. (2023). Unraveling the roles of cerebrospinal fluid-contacting neurons. *eLife*, *12*, e87054. https://doi.org/10.7554/eLife.87054

Xi, Y., Chen, D., Sun, L., Li, Y., & Li, L. (2013). Characterization of zebrafish mutants with defects in bone calcification during development. *Biochemical and biophysical research communications, 440*(1), 132–136. https://doi.org/10.1016/j.bbrc.2013.09.043

Zhang, X., Jia, S., Chen, Z., Chong, Y. L., Xie, H., Feng, D., Wu, X., Song, D. Z., Roy, S., & Zhao, C. (2018). Cilia-driven cerebrospinal fluid flow directs expression of urotensin neuropeptides to straighten the vertebrate body axis. *Nature genetics*, *50*(12), 1666–1673. https://doi.org/10.1038/s41588-018-0260-3